CHARLES UNIVERSITY

FACULTY OF PHARMACY IN HRADEC KRÁLOVÉ

DPT. OF PHARMACEUTICAL CHEMISTRY AND PHARMACEUTICAL ANALYSIS

Design, Synthesis, and Evaluation of Heterocyclic Compounds with Potential Antimicrobial Activity V

Diploma Thesis

Head of Department: prof. PharmDr. Martin Doležal, Ph.D.

Supervisor: Assoc. Prof. PharmDr. Jan Zitko, Ph.D.

Consultant: Ghada Bouz, Ph.D.

Candidate: Asal Askari

Hradec Králové, 2024

Acknowledgement

I would like to thank my supervisor, doc. PharmDr. Jan Zitko, Ph.D., my consultant Ghada Bouz, Ph.D., and our head of department, prof. PharmDr. Martin Doležal, Ph.D. for their guidance and support, and finally my family for their endless love and trust in my abilities.

The study was supported by „The project National Institute of virology and bacteriology (Programme EXCELES, ID Project No. LX22NPO5103) - Funded by the European Union - Next Generation EU.“.

Supported by grant SVV 260 666.

„I declare that this thesis is my original author's work, which has been composed solely by myself (under the guidance of my consultant). All the literature and other resources from which I drew information are cited in the list of used literature and are quoted in the paper. The work has not been used to get another or the same title.“

Name: Asal askari

Hradec Králové, 15.05.2024

TABLE OF CONTENTS

1. LIST OF ABBREVIATIONS

AQs	Antistaphylococcal quinazolones
B. subtilis	*Bacillus subtilis*
CA-MRSA	Community acquired MRSA
CDC	Center for Disease Control and prevention in Atlanta
E. coli	*Escherichia coli*
HA/MRSA	Hospital acquired *Staphylococcus aureus*
LDH	Lactate dehydrogenase
MDR	Multidrug resistance
MRSA	Methicillin-resistant *Staphylococcus aureus*
MSSA	Methicillin-susceptible *Staphylococcus aureus*
PABA	Para-aminobenzoic acid
PBP	Penicillin binding protein
P. aeruginosa	*Pseudomonas aeruginosa*
SA	*Staphylococcus aureus*
TB	Tuberculosis
VISA	Vancomycin-intermediate *Staphylococcus aureus*
VRSA	Vancomycin-resistant *Staphylococcus aureus*
IDSA-ATS	Infectious Diseases Society of America and the American Thoracic Society.

2. AIM OF WORK

Staphylococcus aureus (SA) is one of the most common causes of both common and life-threatening infections.[1] One of the ways to control *SA* infections is to develop new antimicrobials, preferably with distinctive mechanism of actions as an attempt to avoid resistance emergence.[2,3] Quinazolone serves as an interesting backbone for many different biologically active compounds, and antistaphylococcal quinazolones (AQs) have established structure-activity-relationships in the literature. AQs are reported to target penicillin binding protein (PBP), DNA topoisomerase, and lactate dehydrogenase (LDH).[3] With the use of in silico docking, we coupled our wide antibacterial knowledge with what has been described in the literature to design novel, potentially active AQs targeting PBP. We prepared our intermediate compound (2-methyl-4*H*-3,1-benzoxazin-4one) by reacting acetic anhydride with 2-aminobenzoic acid under reflux and heating. Next step was to react the latter product with various substituted benzyl amines to achieve final compounds which is shown in Figure 1. Final compounds were evaluated for their antimicrobial activity against *SA* and -as complementary testing- against other bacteria, fungi, and mycobacteria of clinical importance.

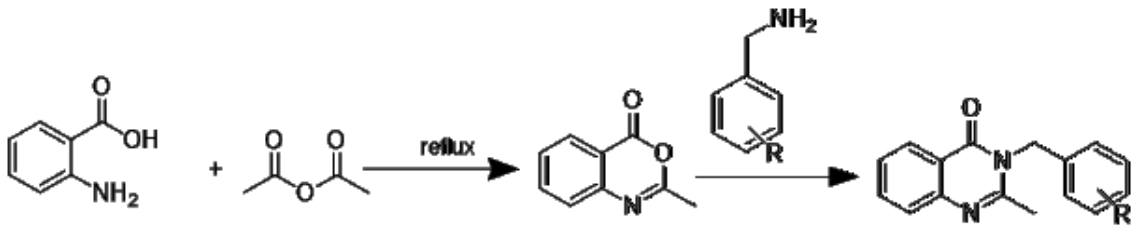

R = 2,4-diMeO; 3-MeO; 4-MeO; 3-F; 2-Me; 3-Cl; 4-CF_3; 2,4-diCl; 3,4-diCl; etc..

Figure 1. The general procedure and structures of final compounds prepared in this diploma.

3. INTRODUCTION & DESIGN RATIONALE

3.1. Staphylococcus aureus (SA) infections

Staphylococcus aureus (*SA*), a Gram - and coagulase-positive coccus, is the causative organism of a number of both common and life-threatening infections, leading to increased morbidity and mortality of afflicted individuals.[4] *SA* colonize about 20–30 % of population mostly in the nose area and also in some other areas, such as the skin, throat, axillae, groin, intestines, etc. Although colonization is not a serious issue, it is a risk factor for various infections that can be a simple or invasive; including osteomyelitis, septicaemia, septic arthritis, infective endocarditis, device-related infections, especially when the immune system of the individual is weakened due to disease or concurrent medication intake Besides, *SA* infections can be classified as acute, chronic or recurrent.[5] Figure 2 demonstrates *SA* cell structure and also a few pathogenic factors. *SA* has a complex cell wall which is made of peptidoglycan thick layer that's covered with a polysaccharide capsule.

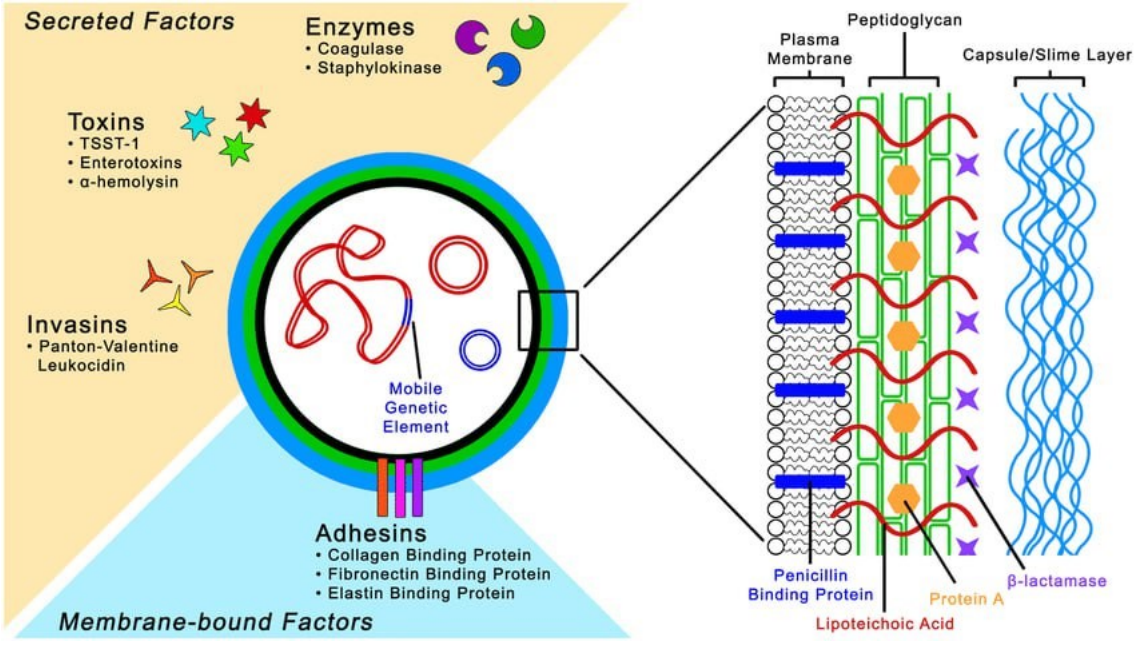

Figure 2. Cell wall structure of *Staphylococcus aureus. Taken from* [6]

Clinically available antistaphylococcal agents include beta-lactams, vancomycin, tetracyclines, among others. Selected examples are mentioned in Table 1 along with their chemical structures and mechanisms of action.

Table 1. Clinically available antistaphylococcal agents.

Agent	Molecular target/MOA	Chemical structure
Vancomycin	Cell wall synthesis inhibitor by attaching to the D-Ala-D-Ala terminal of the growing peptide chain at time of cell wall production.[7]	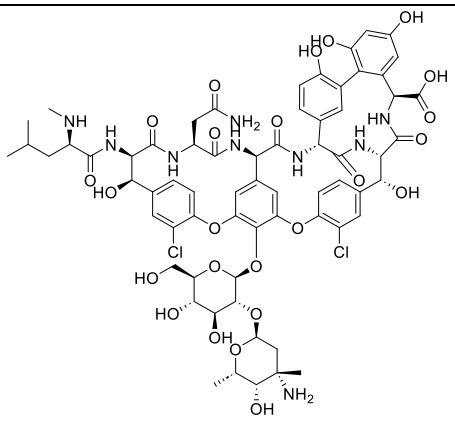
Beta-lactams	Cell wall inhibitors by forming covalent bonds with PBP (penicillin binding proteins) which are enzymes responsible in final steps of peptidoglycan cross linking in both gram-positive and gram-negative bacteria.[8]	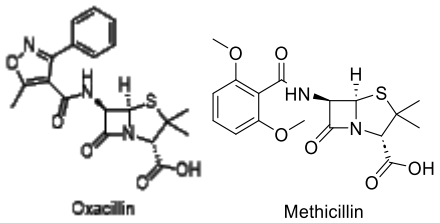 Oxacillin Methicillin
Linezolid	Protein synthesis inhibitor (50S).[9]	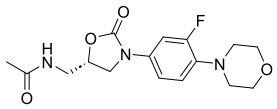
Daptomycin	Forms micelle-like oligomeric form by binding to Ca^{2+} that transports daptomycin to bacterial membrane which in return causes leakage of cystolic content and bactericidal effect.[10]	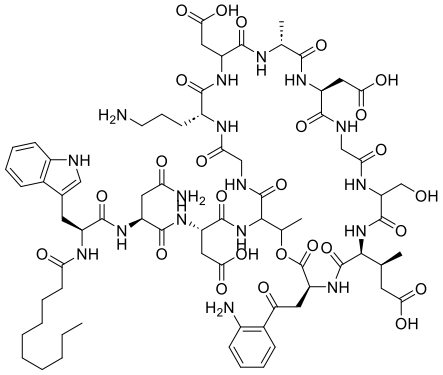
Trimethoprim- sulfamethoxazole	Inhibits dihydrofolate reductase, which is the enzyme responsible for catalyzing the last step of bacterial folic acid synthesis. Sulfamethoxazole is a competitor of p-aminobenzoic acid (PABA), while	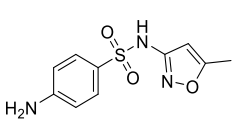 Sulfamethoxazole 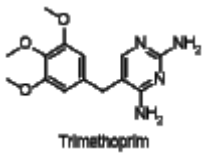 Trimethoprim

	trimethoprim is a direct competitor of the enzyme dihydrofolate reductase. combining these two agents create a synergistic anti-folate effect.[11]	
Macrolides	Protein synthesis inhibitors by inhibiting the 50S ribosome through specific binding to the 23S ribosomal subunit.[12]	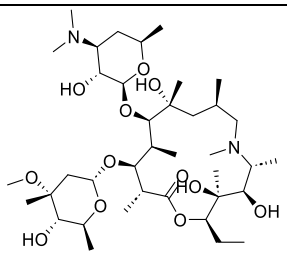 azithromycin
Aminoglycosides	Protein synthesis inhibitors by inhibiting the bacterial 30s ribosomal subunit.[13]	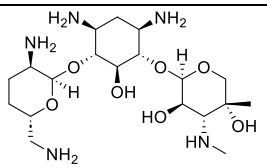 Gentamicin
Fluoroquinolones	Inhibit DNA gyrase and topoisomerase IV activities.[14]	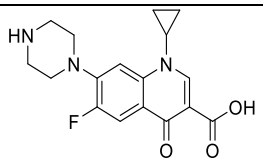 Ciprofloxacin
Clindamycin	Protein synthesis inhibitor by inhibiting to the 50S ribosome.[15]	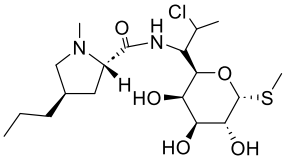
Mupirocin	Mupirocin inhibits bacterial RNA and protein synthesis by binding to bacterial isoleucyl tRNA synthetase, which catalyzes the formation of isoleucyl tRNA from isoleucine and tRNA.24 This prevents incorporation of isoleucine into protein chains, leading to arrest of protein synthesis.[16]	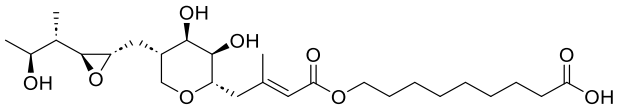

3.2. Antimicrobial resistance

Antibacterials have been used for over 100 years now. This fact along with antibiotics abuse, either overuse without indication or misuse without proper cultures of the causative organism, lead to fast and widespread development of antibiotic resistance worldwide. Resistance to antibacterials happens as fast as the new antibiotics enter the market. The situation is that serious that in the current world almost all known bacteria have already developed resistance to the available antibacterials. There are also some pathogens that can survive and grow even in presence of multiple antibacterial agents which caused arising multi drug resistance (MDR). MDR has caused great concern in worldwide health issues therefore there is a great interest in developing new compounds and novel approaches to overcome this problem.[17]

Below Figures 3, 4 and 5 are from a study on antimicrobial resistance of SA isolated between 2017 and 2022 from infections at tertiary care hospital in Romania that demonstrate antibiotic resistance pattern and also ratio between MRSA and MSSA. MRSA strains were more resistant to all antimicrobials than MSSA strains.

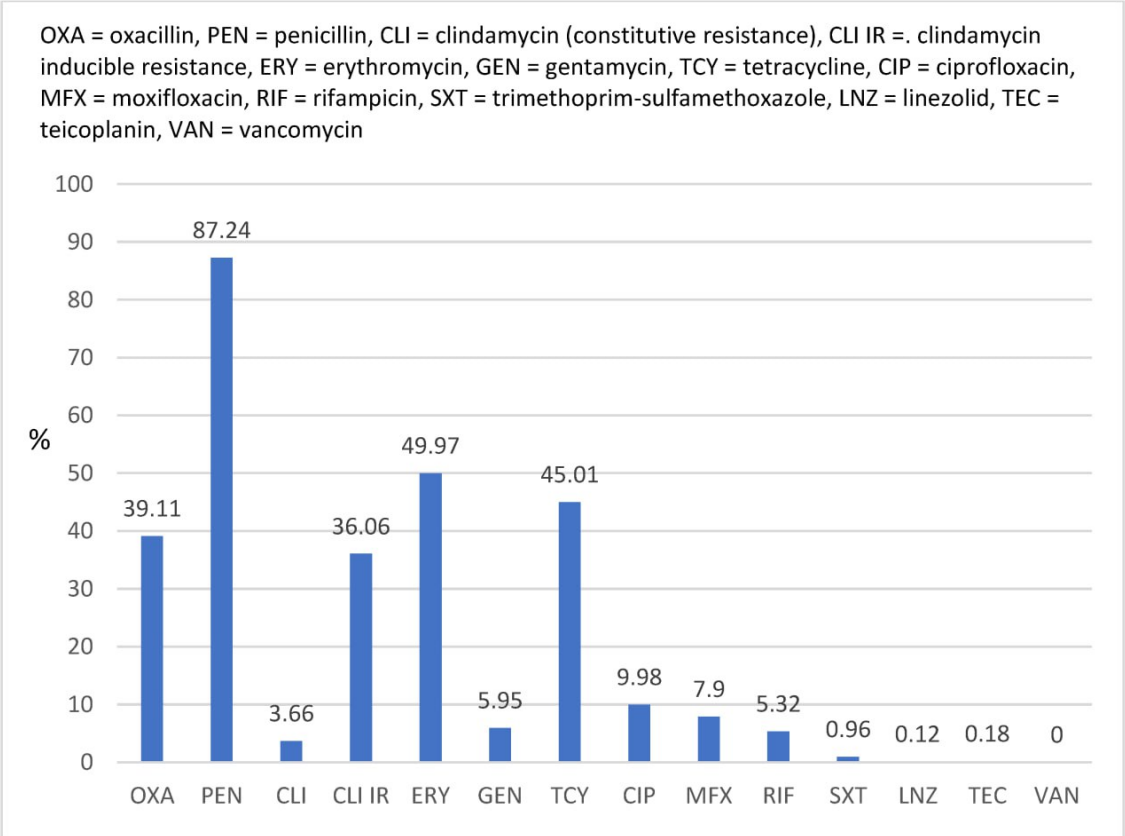

Figure 3. Overall rates of resistance to antimicrobials of *Staphylococcus aureus* strains (N = 1672) isolated between 2017 and 2022 from infections at a tertiary care hospital in Romania (Staphylococci were mostly isolated from wounds (57,78%, followed by blood (18,72%),lower

respiratory tract secretions(9.39%) and then from urine, ear secretions, pleural fluid, and joint fluids Taken from [18]

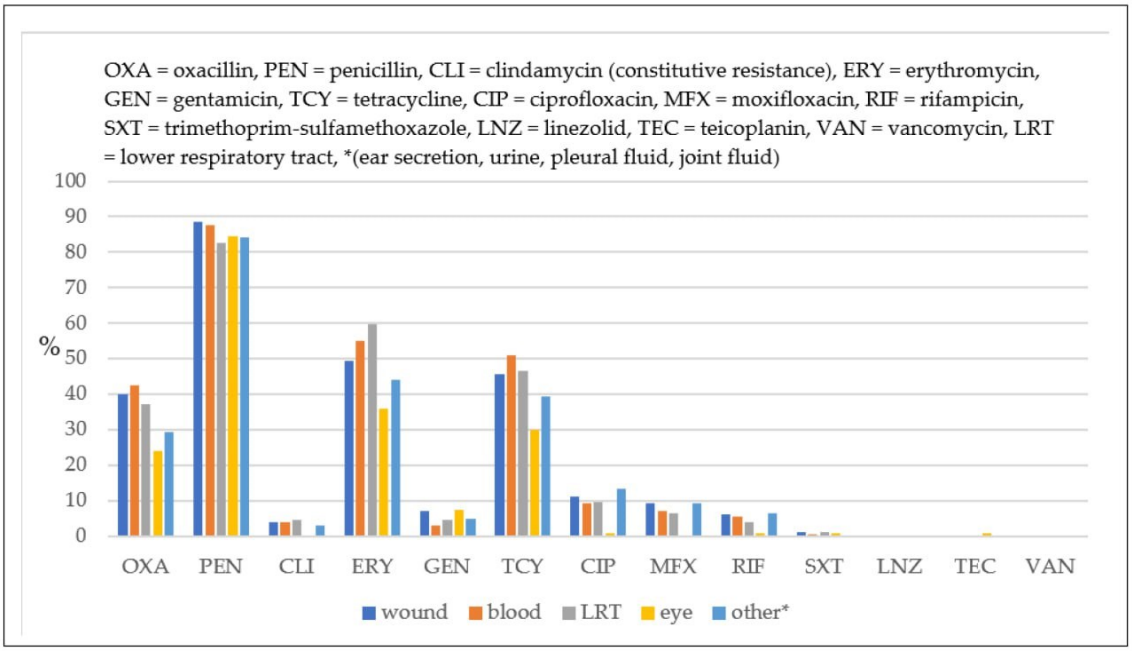

Figure 4. Comparative resistance of *Staphylococcus aureus* strains isolated from different clinical specimens. Taken from [18]

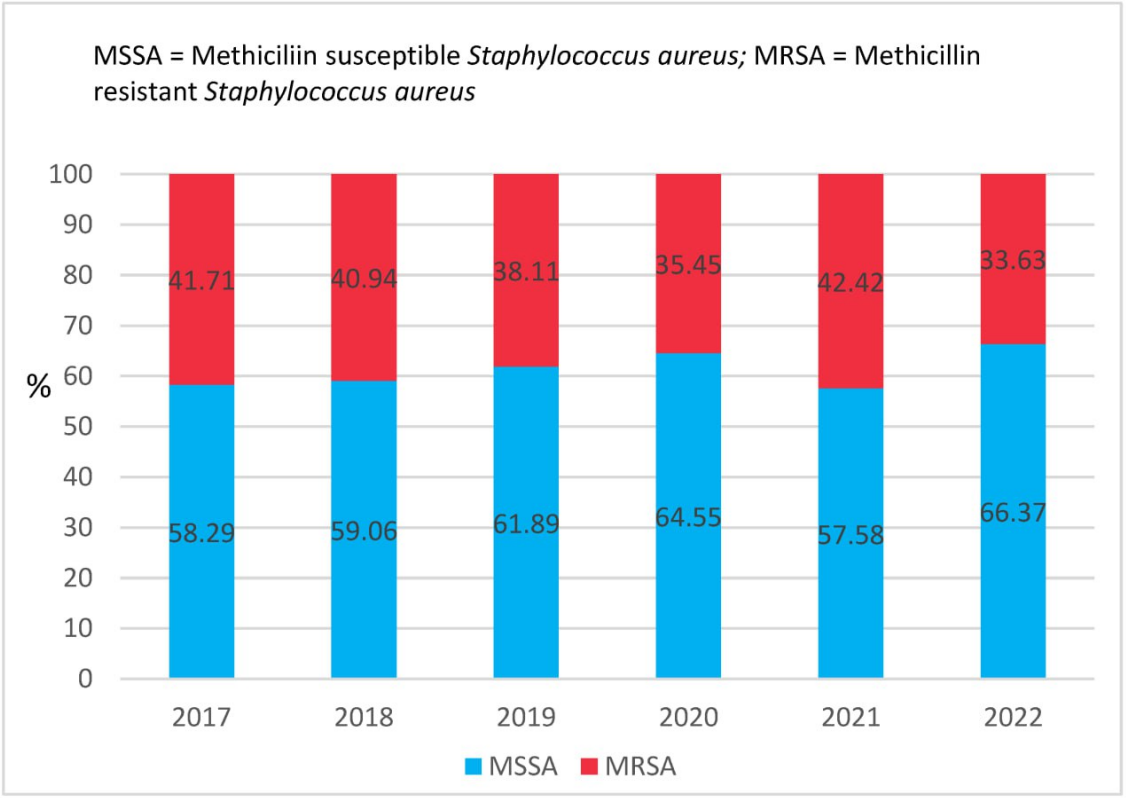

Figure 5. MRSA evolution between 2017 and 2022. Taken from [18]

3.2.1. Resistance mechanisms in *SA*

Microorganisms employ four main defense mechanisms to prevent the effects of antimicrobial agents, in other words to exert resistance.[1,19] These include reducing the medication's intake, altering the drug's target, inactivating the drug, and inducing active efflux. These mechanisms can either be acquired (by the bacteria obtaining them from another bacteria via plasmid, bacteriophage, or simple uptake of DNA containing the necessary genes - present in only certain isolates of a species) or intrinsic (the bacteria already have genes on its chromosome which are natural to all members of a species - these genes just need to be activated).[20,21] The bacteria may use one or both of these methods of gene acquisition, depending on the medication in question.

Greater than any other human pathogen, *SA* can serve as an example of the adaptive evolution of bacteria during the antibiotic era. This is because it has shown a remarkable capacity to rapidly adapt to new antibiotics by developing resistance mechanisms, beginning with penicillin and methicillin and unfortunately continuing with the most recent ones, linezolid and daptomycin.[22,23] The resistance mechanisms of antibiotics include enzymatic inactivation (penicillinase and aminoglycoside-modification enzymes), alteration of the target with decreased affinity for the antibiotic (e.g., D-Ala-D-Lac of peptidoglycan precursors of vancomycin-resistant strains and PBP 2a of methicillin-resistant *S. aureus*), trapping of the antibiotic (for vancomycin and possibly daptomycin) and efflux pumps (fluoroquinolones and tetracycline are notable examples).[24–26] *SA* has gained complex genetic arrays such as the *vanA* operon or staphylococcal chromosomal cassette *mec* elements. Though, resistance to other antibiotics—such as fluoroquinolones, linezolid, and daptomycin—has emerged as a result of spontaneous mutations and positive selection.[22]

Penicillin-resistant *SA* can produce penicillinase, which hydrolyzes the penicillin-lactam ring, resulting in penicillin resistance. Afterwards, researchers synthesized methicillin, a novel semisynthetic penicillin-resistant to penicillinase and β-lactamase degradation.[27–29] Methicillin was used in the clinic in 1959 and proved to be an effective treatment for penicillin-resistant *SA* infections. Whereas in 1961, just two years after methicillin was introduced, British scientist Jevons reported the isolation of an *MRSA* strain; this resistance was caused by a gene encoding the PBP2a or PBP2', which was incorporated into the methicillin-sensitive *SA* chromosomal element Furthermore, MRSA has quickly emerged as the resistant pathogen that is seen most commonly worldwide, encompassing the Middle East, East Asia, North Africa, North America, and Europe.[30] Patients with MRSA have a 64% higher risk of death compared to

those infected with non-resistance strains)[14] MRSA is divided into two categories, according to its initial source: community-acquired *MRSA* (CA-MRSA) and hospital-acquired MRSA (HA-MRSA). The percentage of MRSA acquired in hospitals in China has risen to 50.4%. Furthermore, according to the US Centers for Disease Control (CDC), the fatality rate from MRSA infections has surpassed that of AIDS, Parkinson's disease, and homicide. Therefore, studying *SA*'s molecular properties, which are now the subject of concerns for global public health, can aid in our understanding of the pathogen's prevalence, tracking its evolution, finding new molecular traits, and providing knowledge for the development of novel anti-*S. aureus* medications.[31,32]

3.2.2. Other forms of resistant *SA*

3.2.2.1. Beta-lactam resistance

For beta-lactam antimicrobials against *S. aureus*, the two-way functional transglycolylase-transpeptidase PBP2 is the most prevalent and significant inhibitory target site and inhibition of PBP produces an imbalance in cell wall synthesis.[33] The transfer of disaccharide pentapeptide source material of peptidoglycan from membrane-bound lipid II to budding polysaccharide chains is coordinated by the transglycosylase domain of the enzyme. The transpeptidase-containing domain aids in linking with the glycine cross-bridge of the fourth D-alanine in a chain next to it one of the means of resistance to beta-lactams is utilization of PBPs with low affinity for beta-lactams, there are also other mechanisms involved in decreasing susceptibility to beta-lactams such as degradation of antibiotic by beta-lactamase, decreased permeability of outer membrane.[34,35]

3.2.2.2. Linezolid and tetracycline resistance

Synthetic antibacterial drug linezolid, which is a member of the oxazolidinone family, inhibits the formation of the 70S ribosomal initiation complex by attaching to 50S ribosomal subunits and preventing protein synthesis. It is one of the few antibiotics that rarely develops resistance in *SA*, making it a wise choice for treating *SA* infections. Rarely can resistance development arise, but when it does, it is due to a chromosomal gene mutation that codes for the 23s rRNA.[36,37]

3.2.2.3. Aminoglycoside resistance

When aminoglycosides attach to the 30S ribosomal subunit, they disrupt protein synthesis, which is how they function as bactericidal antimicrobial agents. Aminoglycoside resistance develops as a result of ribosomal subunit mutations. The development of resistance to

aminoglycosides has also been reported to be facilitated by the acquisition of an aminoglycoside modifying enzyme.[38,39]

3.2.2.4. VISA and VRSA

Vancomycin-intermediate *Staphylococcus aureus* (also called VISA) and vancomycin-resistant *Staphylococcus aureus* (also called VRSA) are certain types of antimicrobial-resistant bacteria. Patients with these two kinds of infections might have underlying conditions like diabetes, kidney disease, previous infections, MRSA, recent exposure to antibiotics. *SA* is categorized to VISA and VRSA based on lab results which is defined as MIC (minimum inhibition concentration) and if MIC is 4–8 μg/mL Its classified as VISA and if is more the 16 μg/mL is considered VRSA.[40–42] The others resistance to be named are resistance to fluoroquinolones, macrolides, etc. It must be noted that The World Health Organization has listed *SA,* MRSA, VISA, and VRSA as priority pathogens for novel antistaphylococcal drug development. [43]

3.3. Novel antistaphylococcal agents

Due to the raising issue of *SA* resistance, research and development (R&D) pipeline continues to introduce novel agents, preferably with novel mechanisms of action. Some of the newly approved agents for clinical uses are listed below in Table 2.

Table 2. Selected novel antistaphylococcal agents, their year of approval, structural class, mechanism of action, and chemical structure.[44]

Agent (year of approval by FDA)	**Structural class**	**MOA**	**Structure**
Lefamulin (2019)	Pleuromutilin derivative	Inhibits protein synthesis via interaction with the 50S ribosomal subunit	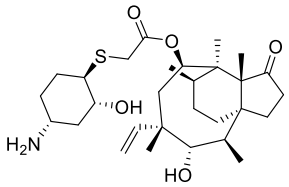
Sarecycline (2018)	Tetracycline	nhibits mRNA translation via interaction with 30S ribosomal subunit, thus Inhibiting protein synthesis	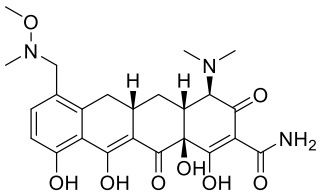
Eravacycline (2018)	Tetracycline	Interacts with the 30S ribosomal subunit thus inhibiting protein synthesis	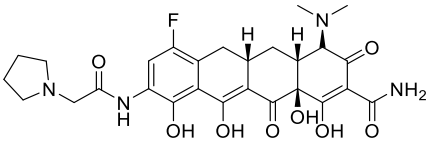
Omadacycline (2018)	Tetracycline	Inhibits protein synthesis by Interacting with the 30S ribosomal subunit	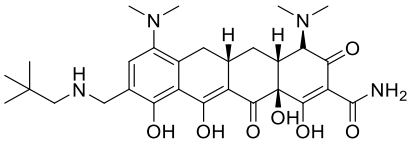
Delafloxacin (2017)	Fluoroquinolone	Inhibits nucleic acid synthesis by inhibition of bacterial DNA gyrase and topoisomerase IV,	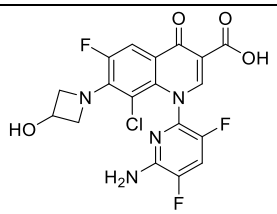
Ozenoxacin (2017)	Quinolone	Inhibits nucleic acid synthesis via inhibition of bacterial DNA gyrase and topoisomerase IV	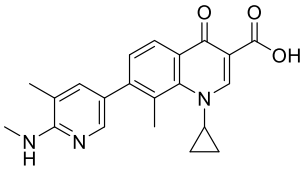
Finafloxacin (2014)	Fluoroquinolone	Inhibits nucleic acid synthesis via inhibition of bacterial type II topoisomerase enzymes, DNA gyrase	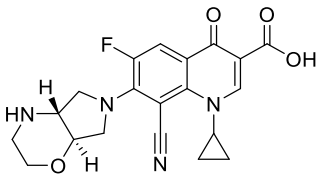

		and topoisomerase IV	
Solithromycin (2016)	Fluoroketolide	Binds to the 50S ribosomal subunit, thus inhibits protein synthesis	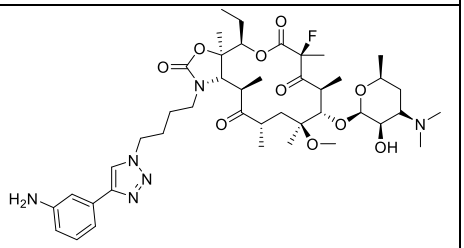
Tedizolid (FDA in 2014 and the EU in 2015)	Oxazolidinone	Binds to the 50S ribosomal subunit, thus inhibits protein synthesis	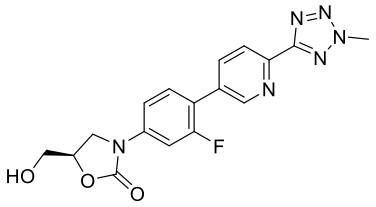
Dalbavancin (2014)	Teicoplanin derivative	Inhibits bacterial cell wall synthesis	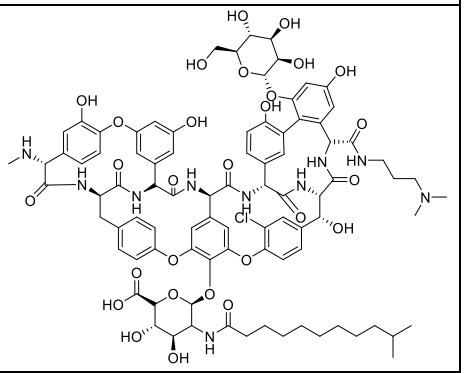
Teicoplanin (2009 for cSSSI; 2013 for hospital acquired and ventilation associated pneumonia)	Glycopeptide	Inhibits bacterial cell wall synthesis	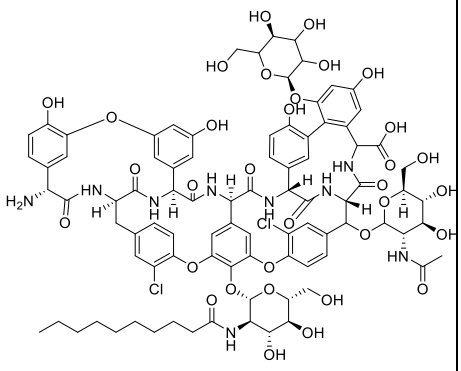

3.4.Quinazolinones

3.4.1. Chemistry

Quinazolinones and quinazolines belong to the important heterocyclic scaffolds in medicinal chemistry. (Figure 6). Quinazoline was first synthesized by Gabriel in 1903 and since then it has shown a remarkable variety of antibacterial, antifungal, anti-inflammatory, anti-malarial, anti-viral, and anti-tubercular activities. In addition, it has some other biological effects like sedative, anti-tumor, hypoglycemic, and anti-convulsant.[45]

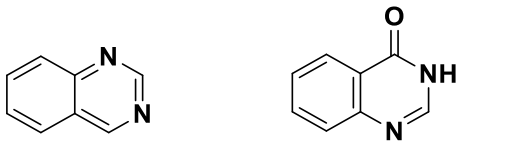

quinazoline quinazolin-4(3*H*)-one

Figure 6. The chemical structures of quinazoline and quinazolin-4(3*H*)-one.

Even though quinazolinone chemistry is thought to be well-established, newer and more complicated quinazolinone structural derivatives are continuously being prepared on a daily basis. Quinazolinones have a significant lactam-lactim tautomeric interaction. in addition, when the methyl group is present in the 2-position, the tautomeric effect is extended and results in the generation of an exo methylene carbon. These observations also demonstrate the existence of this tautomeric interaction. (Figure 7)

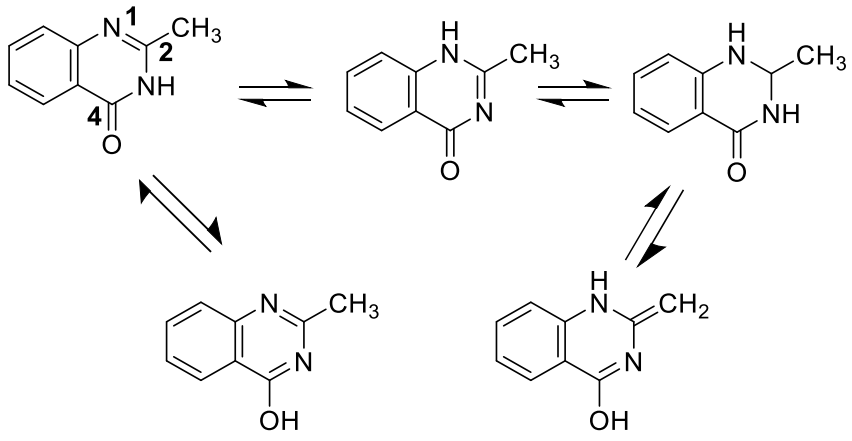

Figure 7. Tautomerism of quinazolinones.

The tautomeric effects that are sustained lead to an increase in the reactivity of substituted-4-(3*H*)-quinazolinones. Quinazolinones are therefore thought of as a "privileged structure" for drug discovery and development.

Regarding stability, it has previously been discovered and documented that the quinazolinone ring exhibits a high degree of stability in the face of oxidation, reduction, and hydrolysis

processes. To date, no processes involving ring destruction through simple chemical oxidation have been reported.[45]

3.4.2. Quinazoline-containing drugs available in the market

Drugs containing quinazoline core are widely recognized as part of different therapeutic classes of various biological activities. This quick progress suggests that other quinazoline derivatives may soon be undergoing clinical trials.

Methaqualone, the first renowned quinazoline medicine to be marketed, has been used since 1951 for its sedative-hypnotic properties. Many quinazoline derivatives are currently patented and on the market as possible treatments for a range of illnesses. A few commercially available quinazoline containing medications for the treatment of different illnesses are included in the Figure below (Figure 8).[46,47]

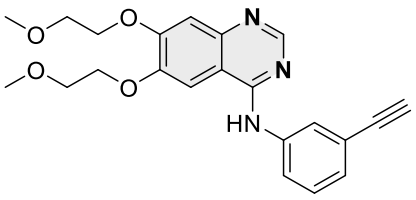

Erlotinib

EGFR inhibitors

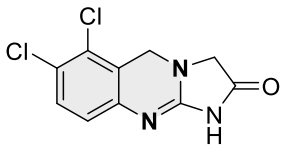

Anagrelide

treatment of essential thrombocytosis & myieloid leukemia

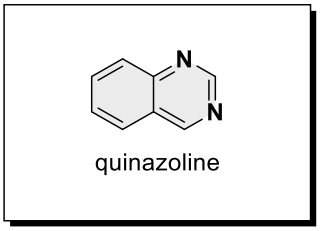

quinazoline

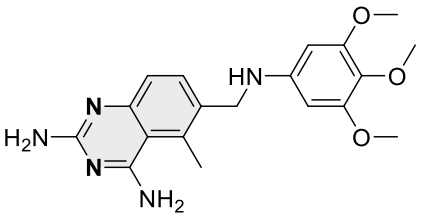

Trimetrexate

DHFR inhibitor

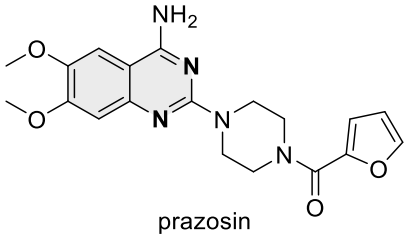

prazosin

Alpha-1 blocker

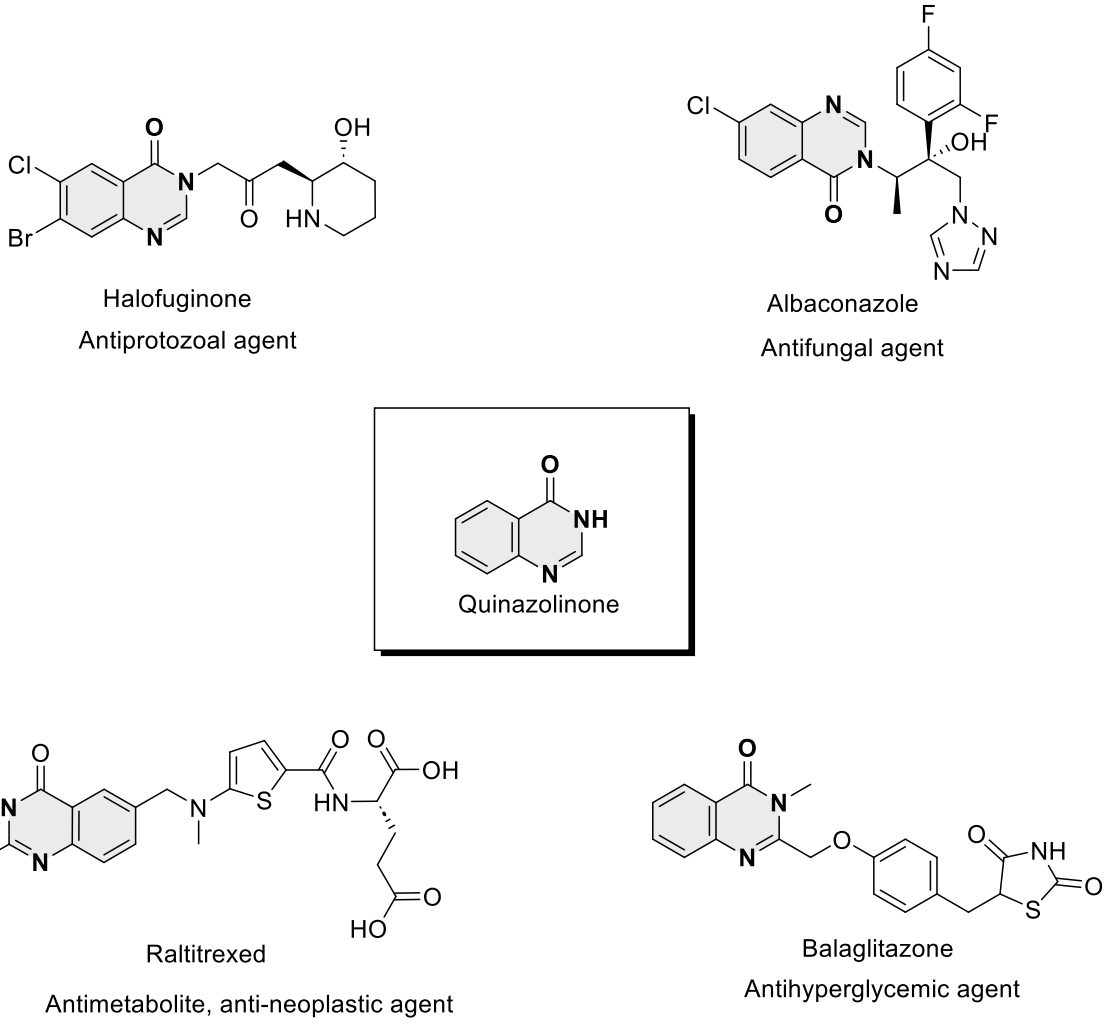

Figure 8. The chemical structures of different quinazoline/quinazolinone-containing drugs with various pharmacological effects.

3.4.3. Antistaphylococcal Quinazolinones

Based on literature search of original experimental papers reporting the design, synthesis, and antistaphylococcal activity of quinazolinones, the structure-activity-relationships of PBP 2a-targeting quinazolinone can be summarized as in Figure 9 below.

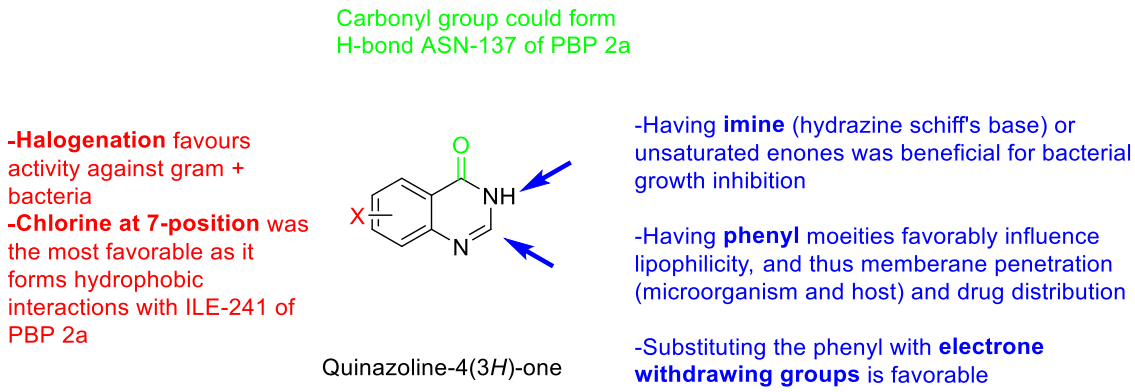

Figure 9. The structure-activity-relationship of antistaphylococcal quinazolinones targeting PBP 2a.

Studies on Quinazoline-4-(3*H*)-one derivatives including synthesis, antimicrobial and docking studies among the synthesized products shows 3-benzyl-2-(4-chlorophenyl)quinazoline-4(3*H*)one has the highest in vitro antimicrobial activity, namely against *S. aureus, B. subtilis*, *P. aeruginosa* and *E. coli (refer to Figure 10).*[48]

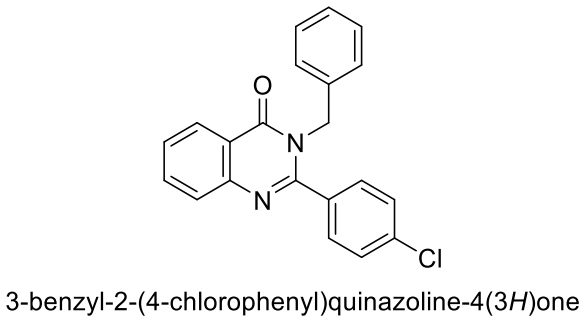

Figure 10. One of the novel quinazoline derivatives with potent antimicrobial activity.

Studies show that disubstituted 2,4 diaminoquinazolines have a strong effect against both Gram + and Gram - pathogens (Figure 11).[49]

Notably studies have been evaluating the potency for synergistic activity of a lead quinazolinone with a few antibiotics of different classes and as a result it shows the quinazolinone synergized with β-lactam antibiotics. Combining the quinazolinone with commercial piperacillin-tazobactam showed bactericidal synergism at sub-MICs of all three. According to the implied

mechanism, the synergistic effect in MRSA is caused by tazobactam inhibiting the β-lactamase, which shields piperacillin from hydrolysis, and which can then inhibit its target. In addition, quinazolinone binds to PBP 2a's allosteric site, inducing the allosteric response. As a result, the active site opens and binds to another piperacillin molecule. Stated differently, PBP 2a, which is typically not inhibited by piperacillin, becomes susceptible to inhibition when quinazolinone is present. The overall result is an impairment in the synthesis of cell walls, resulting in bactericidal effects.[50]

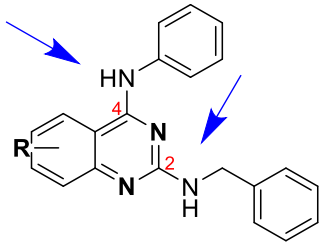

R= 6-Cl, 6-Br, 7-Cl, 7-Br, 6-OMe, 6-Me, 7-Me

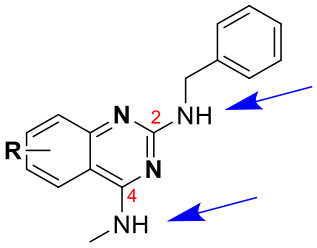

R= 6-Cl, 7-Cl, 7-Br, 6-OMe, 6-Me, 7-Me

Figure 11. Structure of N^2,N^4-disubstituted quinazoline-2,4-diamines.

Studies on 2-styrylquinazolinone (Figure 12) derivatives have shown that 3-*N*-phenyl with ortho para or meta position has a significant impact on antibacterial activity.[51] Styryl group at position C-2 is known to be essential for inhibitory activity. Substitution of H with flouro group at C-5 is favorable for antibacterial activity. however, chloro group was not favored. Substitution at position 6 and 7 were also found to be useful. All together, 2-styrylquinazolinone derivatives have shown potential to be used as novel effective antibacterial agents in the future.[51]

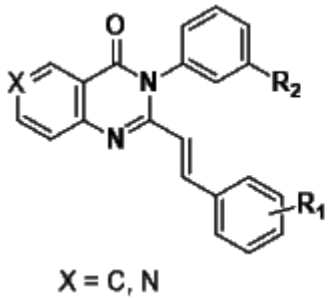

R^1 = 4-Cl; R^2 = OH; MIC = 0.125 µg/ml (*SA*)
R^1 = 4-F; R^2 = OH; MIC = 0.25 µg/ml (*SA*)
R^1 = 4-NO2; R^2 = OH; MIC = 0.25 µg/ml (*SA*)
R^1 = 4-CN; R^2 = OH; MIC = 0.03 µg/ml (*SA*)
R^1 = 4-Me; R^2 = OH; MIC = 025 µg/ml (*SA*)
R^1 = 4-Et; R^2 = OH; MIC = 0.5 µg/ml (*SA*)

Figure 12. 2-Styrylquinazolinone derivatives with antibacterial activity.

3.5. Design rationale

Based on the SARs of antistaphylococcal quinazolinones targeting bacterial PBP 2a, we designed a preliminary general structure shown in Figure 13 below. Then we performed *in silico* docking into the active site of the target enzyme (PDB id: 6Q9N), where we identified conventional intramolecular hydrogen bonding. This work is part of a larger series of compounds based on in silico docking study. The main difference between them is the linker; methylene (main focus of this diploma work), imine, carbonyl, and urea.

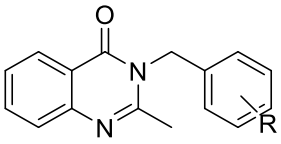

R=2,4-diMeO; 3-MeO; 4-MeO; 3-F; 2-Me; 3-Cl; 4-CF_3; 2,4-diCl; 3,4-diCl; etc..

Figure 13. The general structure of compounds included in this diploma work.

All final compounds were evaluated for their antistaphylococcal activity and as complementary testing, they were screened for antibacterial activity against *Staphylococcus epidermidis*, *Enterococcus faecalis*, *Escherichia coli*, *Klebsiella pneumonia*, *Serratia marcescens*, *Pseudomonas aeruginosa*; antimycobacterial activity against *Mtb H37R*, *M. kansasii*, *M. avium*, *Mtb* H37Ra, *M. smegmatis* , *M. aurum*; and antifungal activity against *Candida albicans*, *Candida krusei*, *Candida parapsilosis*, *Candida tropicalis, Aspergillus fumigatus, Aspergillus flavus*, *Lichtheimia corymbifera*, *Trichophyton interdigitale*. Compounds are ordered throughout the text in an ascending order based on their lipophilicity (log *P* value).

4. EXPERIMENTAL PART

4.1. Instrumentation

Most of the chemical reactions were carried in normal laboratory glass equipment and at room temperature.

The progress of the reaction was checked by Thin Layer Chromatography (TLC) (Alugram® Sil G/UV254, Machery-Nagel, Postfach, Germany) with UV detection using wavelength 254 nm.

For selected compounds, microwave-assisted reactions were performed in a CEM Discover microwave reactor with a focused field (CEM Corporation, Matthews, NC, USA) connected to an Explorer 24 autosampler (CEM Corporation).

Flash chromatography of the final compounds was performed on a puriFlash XS420+ (Interchim, Montluçon, France) with original columns (spherical silica, 30 µm) provided by the same company. The mobile phase was ethyl acetate (EtOAc) in hexane (Hex), gradient elution 0–100%, and detection was performed by UV-VIS detector at 254 nm and 280 nm. NMR spectra of prepared compounds were recorded on Varian VNMR S500 (499.87 MHz for ^{1}H and 125.71 MHz for ^{13}C) spectrometer (Varian Corporation, Palo Alto, CA, USA).

Infrared spectra were recorded with spectrometer FT-IR Nicolet 6700 (Thermo Scientific, Waltham, MA, USA) using attenuated total reflectance (ATR-Ge) methodology.

Elemental analysis will be carried out using a vario Micro Cube Elemental Analyzer (Elementar Analysensysteme GmbH, Hanau, Germany).

Melting points were assessed by SMP30 Stuart Scientific (Bibby Sterling Ltd., Staffordshire, UK) in open capillary.

Lipophilicity parameter log *P* were calculated by software ChemDraw Professional 22.2 (CambridgeSoft, Cambridge, MA, USA).

4.2. Chemistry

4.2.1. General Procedure

2-Methylquinazolin-4(3*H*)-one

The first step is the synthesis of the starting material by reacting acetic anhydride (50 mL in excess) with 2-aminobenzoic acid (3.98 g; 39 mmol) under reflux and heating (130 °C) for 4 hours. The liquids were evaporated under reduced pressure, and the crude product was recrystallized from hexane (500 mL) and traces of EtOAc (1 mL). Crystals were filtered off and left to dry. This step was repeated as needed to scale up.

Final products

Final products were prepared by reacting 2-methyl-4*H*-benzo[d][1,3]oxazin-4-one (644 mg); 2 mmol, referred to as reactant 1 in Table 3 with corresponding benzyl amine 1.2 equivalent (referred to as reactant 2 in Table3, in 10 mL of ethanol as solvent under reflux (80 °C) for 24 hours as shown in Figure 14. This is a classic aminolysis reaction where the lactone reacts with an amine to form a lactam. The reaction was stopped and extracted by adding EtOAc as little as needed (30 mL). Acidic distilled water (water with 10% HCl) was then added (30 mL) and the two phases were mixed vigorously at room temperature and then transferred to a 500 mL separating funnel. The two layers were then allowed to settle and were separated into two 250 mL beakers. The aqueous layer was rewashed with EtOAc (2 x 30 mL). The combined organic layers from all extractions were then washed one last time with distilled water (100 mL) and then with brine (30 mL). The final organic layer was then transferred to a 150 mL beaker (or less based on the obtained overall volume) and stirred with magnesium sulfate (4 mmol, 500 mg) as a desiccant for 10 min at room temperature. Finally, the dispersion was filtrated through cotton and the resulting filtrate was adsorbed to silica gel and purified using Flash chromatography using gradient elution 0 to 100% EtOAc in hexane. Reactions were monitored by TLC using hexane – ethyl acetate 2:1 mobile phase system. Yields are calculated after all purification steps.

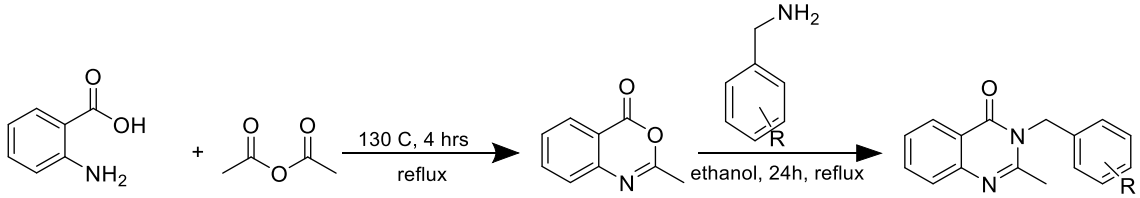

R=2,4-diMeO; 3-MeO; 4-MeO; 3-F; 2-Me; 3-Cl; 4-CF3; 2,4-diCl; 3,4-diCl; etc..

Figure 14. General reaction for synthesis of final compounds

Table 3. Exact quantities used of reactant 1 (2-methyl-4*H*-benzo[*d*][1,3]oxazin-4-one), and reactant 2 (corresponding benzyl amine), with the yield of final compounds.

Code	Reactant 1		Reactant 2			Isolated yield	
	n (mmol)	m (mg)	R	n (mmol)	m (mg)	m (mg)	% to theoretical
GDM-12	2	323	2,4-diMeO	2.4	401.	143	23
GDM-15	2	323	3-MeO	2.4	329.	168	30
GDM-14	2	323	4-MeO	2.4	329.	213	38
GDM-4	2	323	3-F	2.4	300.	107	20
GDM-13	2	323	2-Me	2.4	291	296	56
GDM-10	2	323	3-Cl	2.4	340	279	49
GDM-7	2	323	4-CF3	2.4	392	382	60
GDM-N	2	323	naphthyl	2.4	341	529	88
GDM-2	2	323	3-CF3, 5-F	2.4	463	511	76
GDM-8	2	323	2,4-diCl	2.4	422	294	46
GDM-9	2	323	3,4-diCl	2.4	422	367	56

4.2.2. Final Compounds

Smiles of Final Compounds

Code	Smiles
GDM-12	O=C1N(CC2=CC=C(OC)C=C2OC)C(C)=NC3=C1C=CC=C3
GDM-15	COC1=CC(CN2C(C)=NC3=C(C=CC=C3)C2=O)=CC=C1
GDM-14	COC1=CC=C(CN2C(C)=NC3=C(C=CC=C3)C2=O)C=C1
GDM-4	O=C1N(CC2=CC=CC(F)=C2)C(C)=NC3=C1C=CC=C3
GDM-13	CC1=CC=CC=C1CN2C(C)=NC3=C(C=CC=C3)C2=O
GDM-10	O=C1N(CC2=CC=CC(Cl)=C2)C(C)=NC3=C1C=CC=C3
GDM-7	O=C1N(CC2=CC=C(C(F)(F)F)C=C2)C(C)=NC3=C1C=CC=C3
GDM-N	CC(N1CC2=CC=C3C=CC=CC3=C2)=NC4=C(C=CC=C4)C1=O
GDM-2	FC(F)(C1=CC(F)=CC(CN2C(C)=NC3=C(C=CC=C3)C2=O)=C1)F
GDM-8	O=C1N(CC2=CC=C(Cl)C=C2Cl)C(C)=NC3=C1C=CC=C3
GDM-9	O=C1N(CC2=CC=C(Cl)C(Cl)=C2)C(C)=NC3=C1C=CC=C3

4.2.2.1. 3-(2,4-dimethoxybenzyl)-2-methylquinazolin-4(3H)-one

Code: GDM-12

Chemical structure:

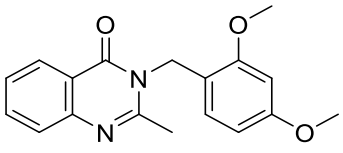

Chemical Formula: $C_{18}H_{18}N_2O_3$

Molecular weight: 310.35 g/mol

Yield: 23%

Appearance: white solid

m.p.: 180–182 °C

R_f (hexane/ EtOAc 2:1): 0.3

Log *P*: 2.69

^{1}H NMR: (600 MHz, DMSO-d_6) δ 8.10 – 8.06 (m, 1H), 7.80 – 7.74 (m, 1H), 7.58 (d, *J* = 8.0 Hz, 1H), 7.46 (t, *J* = 7.5 Hz, 1H), 6.62 – 6.57 (m, 2H), 6.41 – 6.36 (m, 1H), 5.15 (s, 2H, CH_2), 3.81 (s, 3H, OCH_3), 3.69 (s, 3H, OCH_3), 2.42 (s, 3H, CH_3).

^{13}C NMR: (151 MHz, DMSO-d_6) δ 161.94, 160.41, 157.86, 155.82, 147.69, 134.96, 127.14, 127.05, 126.90, 126.86, 120.43, 116.46, 105.45, 99.07, 56.13, 55.75, 42.35, 23.07.

IR: (ATR-Ge, cm^{-1}) 2996 (C–H stretch), 1673 (C=O carbonyl stretch), 1590, 1568 (C–C aromatic stretch).

Elemental analysis: Calculated: 69.66% C; 5.85% H; 9.03% N; 15.47% O. Found: 69.88% C; 5.63% H; 9.14% N; 15.36% O.

4.2.2.2. 3-(3-methoxybenzyl)-2-methylquinazolin-4(3H)-one

Code: GDM-15

Chemical structure:

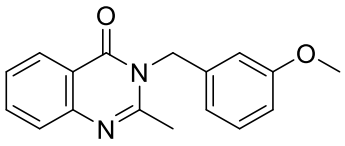

Chemical Formula: $C_{17}H_{16}N_2O_2$

Molecular weight: 280.33 g/mol

Yield: 30%

Appearance: white solid

m.p.: 179–180 °C

R_f (Hexane/ EtOAc 2:1): 0.4

Log *P*: 2.82

^{1}H NMR: (600 MHz, DMSO-d_6) δ 8.14 – 8.09 (m, 1H), 7.81 – 7.75 (m, 1H), 7.58 (d, *J* = 8.1 Hz, 1H), 7.48 (t, *J* = 7.5 Hz, 1H), 7.21 (t, *J* = 7.9 Hz, 1H), 6.84 – 6.79 (m, 1H), 6.74 (t, *J* = 2.1 Hz, 1H), 6.66 (d, *J* = 7.5 Hz, 1H), 5.31 (s, 2H, CH_2), 3.68 (s, 3H, OCH_3), 2.45 (s, 3H, CH_3).

^{13}C NMR: (151 MHz, DMSO-d_6) δ 162.03, 160.11, 155.68, 147.66, 138.69, 135.07, 130.54, 127.18, 127.00, 126.97, 120.38, 118.66, 113.02, 112.91, 55.58, 46.80, 23.44.

IR: (ATR-Ge, cm^{-1}) 3065 (C–H stretch), 1674 (C=O carbonyl stretch), 1599, 1571 (C–C aromatic stretch).

Elemental analysis: Calculated: 72.84% C; 5.75% H; 9.99% N. Found: 72.90% C; 5.69% H; 9.84% N.

4.2.2.3. 3-(4-methoxybenzyl)-2-methylquinazolin-4(3H)-one

Code: GDM-14

Chemical structure:

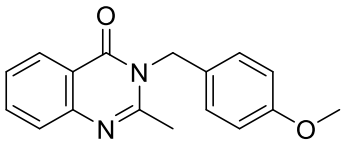

Chemical Formula: $C_{17}H_{16}N_2O_2$

Molecular weight: 280.33 g/mol

Yield: 38%

Appearance: white solid

m.p.: 177–179 °C

R_f (Hexane/ EtOAc 2:1): 0.4

Log P: 2.82

^{1}H NMR: (600 MHz, DMSO-d_6) δ 8.12 – 8.08 (m, 1H), 7.83 – 7.77 (m, 1H), 7.61 (d, *J* = 7.9 Hz, 1H), 7.51 – 7.46 (m, 1H), 7.22 (d, *J* = 7.4 Hz, 1H), 7.16 – 7.10 (m, 1H), 7.08 – 7.02 (m, 1H), 6.52 (d, *J* = 7.7 Hz, 1H), 5.27 (s, 2H, CH_2), 3.40 (s, 3H), 2.36 (s, 3H).

^{13}C NMR: 161.60, 158.61, 154.62, 146.93, 133.43, 130.50, 128.60, 127.34, 126.81, 126.70, 120.34, 114.12, 114.12, 55.81, 45.30, 22.90.

IR: (ATR-Ge, cm^{-1}) 2996 (C–H stretch), 1669 (C=O carbonyl stretch), 1596, 1570, 1557 (C–C aromatic stretch).

Elemental analysis: Calculated: 72.84% C; 5.75% H; 9.99% N. Found: 72.62% C; 5.97% H; 9.88% N.

4.2.2.4. 3-(3-fluorobenzyl)-2-methylquinazolin-4(3*H*)-one

Code: GDM-4

Chemical structure:

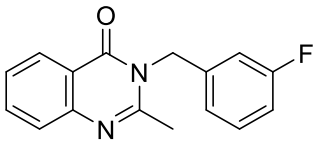

Chemical Formula: $C_{16}H_{13}FN_2O$

Molecular weight: 268.29 g/mol

Yield: 20%

Appearance: white solid

m.p.: 170–172 °C

R_f (Hexane/EtOAc 2:1): 0.5

Log *P*: 3.1

^{1}H NMR: (600 MHz, $CDCl_3$) δ 8.30 – 8.26 (m, 1H), 7.76 – 7.70 (m, 1H), 7.62 (d, *J* = 8.0 Hz, 1H), 7.45 (t, *J* = 7.4 Hz, 1H), 7.32 – 7.24 (m, 2H), 6.98 – 6.91 (m, 1H), 6.91 – 6.86 (m, 1H), 5.36 (s, 2H, CH_2), 2.52 (s, 3H, CH_3).

^{13}C NMR: (151 MHz, $CDCl_3$) δ 164.08, 162.45, 154.35, 147.43, 138.58, 134.66 (q, *J* = 32 Hz), 130.86, 130.66, 126.92, 126.79 (q, *J* = 272.4 Hz), 122.18, 120.38, 114.92 (q, *J* = 6 Hz), 113.66 (q, *J* = 4 Hz), 46.80, 23.45.

IR: (ATR-Ge, cm^{-1}) 3057 (C–H stretch), 1671 (C=O carbonyl stretch), 1613, 1596, 1572 (C–C aromatic stretch).

Elemental analysis: C, 71.63; H, 4.88; N, 10.44

4.2.2.5. 2-methyl-3-(2-methylbenzyl)quinazolin-4(3H)-one

Code: GDM-13

Chemical structure:

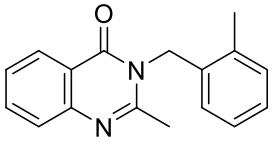

Chemical Formula: $C_{17}H_{16}N_2O$

Molecular weight: 264.33 g/mol

Yield: 56%

Appearance: yellow solid

m.p.: 172–174 °C

R_f (Hexane/ EtOAc 2:1): 0.5

Log *P*: 3.43

^{1}H NMR: (600 MHz, $CDCl_3$) δ 8.28 (dd, *J* = 6.4, 0.6 Hz, 1H), 7.78 – 7.72 (m, 1H), 7.65 (d, *J* = 7.7 Hz, 1H), 7.48 – 7.44 (m, 1H), 7.16 (t, *J* = 8.0 Hz, 2H), 7.10 – 7.04 (m, 1H), 6.68 – 6.63 (m, 1H), 5.32 (s, 2H , CH_2), 2.48 (s, 3H, CH_3), 2.41 (s, 3H, CH_3).

^{13}C NMR: (151 MHz, $CDCl_3$) δ 162.35, 154.80, 147.53, 134.55, 133.52, 132.80, 130.66, 128.66, 128.23, 127.25, 123.92, 122.75, 121.66, 120.38, 44.99, 23.13, 19.24.

IR: (ATR-Ge, cm^{-1}) 3070 (C–H stretch), 1673 (C=O carbonyl stretch), 1603, 1592, 1570 (C–C aromatic stretch).

Elemental analysis: Calculated: 77.25% C; 6.10% H; 10.60% N. Found: 77.11% C; 6.24% H; 10.65% N.

4.2.2.6. 3-(3-chlorobenzyl)-2-methylquinazolin-4(3H)-one

Code: GDM-10

Chemical structure:

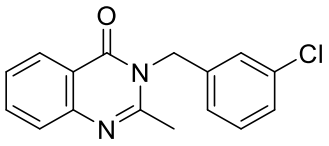

Chemical Formula: $C_{16}H_{13}ClN_2O$

Molecular weight: 284.74 g/mol

Yield: 49%

Appearance: yellow solid

m.p.: 171–172 °C

R_f (Hexane/ EtOAc 2:1): 0.5

Log *P*: 3.5

^{1}H NMR: (600 MHz, DMSO-d_6) δ 8.13 – 8.09 (m, 1H), 7.81 – 7.76 (m, 1H), 7.61 – 7.56 (m, 1H), 7.51 – 7.45 (m, 1H), 7.36 – 7.29 (m, 2H), 7.28 (d, *J* = 2.0 Hz, 1H), 7.13 – 7.08 (m, 1H), 5.33 (s, 2H, CH_2), 2.45 (s, 3H, CH_3).

^{13}C NMR: (151 MHz, DMSO-d_6) δ 162.06, 155.49, 147.65, 139.67, 135.13, 133.98, 131.26, 127.93, 127.21, 127.05, 126.96, 126.93, 125.50, 120.39, 46.56, 23.51.

IR: (ATR-Ge, cm^{-1}) 3010 (C–H stretch), 1672 (C=O carbonyl stretch), 1638, 1594, 1571 (C–C aromatic stretch).

Elemental analysis: Calculated: 67.49% C; 4.60% H; 9.84% N. Found: 67.39% C; 4.55% H; 9.87% N.

4.2.2.7. 2-methyl-3-(4-(trifluoromethyl)benzyl)quinazolin-4(3H)-one

Code: GDM-7

Chemical structure:

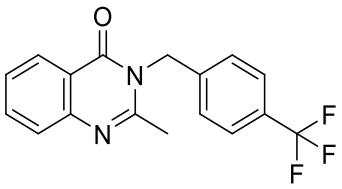

Chemical Formula: $C_{17}H_{13}F_3N_2O$

Molecular weight: 318.30 g/mol

Yield: 60%

Appearance: white solid

m.p.: 174–176 °C

R_f (Hexane/ EtOAc 2:1): 0.6

Log *P*: 3.86

^{1}H NMR: (600 MHz, DMSO-d_6) δ 8.20 – 8.16 (m, 2H), 7.89 – 7.84 (m, 2H), 7.57 – 7.52 (m, 2H), 7.17 – 7.11 (m, 2H), 4.28 (s, 2H, CH_2), 2.08 (s, 3H, CH_3).

^{13}C NMR

IR: (ATR-Ge, cm^{-1}) 3066 (C–H stretch), 1656 (C=O carbonyl stretch), 1592, 1569, 1516 (C–C aromatic stretch).

Elemental analysis: Calculated: 64.15% C; 4.12% H; 8.80% N.

4.2.2.8. 2-methyl-3-(naphthalen-2-ylmethyl)quinazolin-4(3H)-one

Code: GDM-N

Chemical structure:

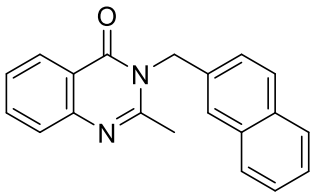

Chemical Formula: $C_{20}H_{16}N_2O$

Molecular weight: 300.36 g/mol

Yield: 88%

Appearance: white solid

m.p.: 178–179 °C

R_f (Hexane/ EtOAc 2:1): 0.6

Log P: 3.94

^{1}H NMR: (600 MHz, $CDCl_3$) δ 8.32 – 8.28 (m, 1H), 8.06 – 8.00 (m, 1H), 7.94 – 7.87 (m, 1H), 7.81 – 7.74 (m, 2H), 7.71 – 7.67 (m, 1H), 7.64 – 7.44 (m, 2H), 7.43 – 7.28 (m, 2H), 6.84 – 6.80 (m, 1H), 5.82 (s, 2H, CH_2), 2.47 (s, 3H, CH_3).

^{13}C NMR: (151 MHz, $CDCl_3$) δ 169.13, 168.82, 162.37, 154.98, 147.55, 139.76, 134.65, 133.87, 132.75, 130.74, 129.03, 128.18, 126.96, 125.62, 123.34, 122.72, 121.57, 120.38, 44.86, 23.13.

IR: (ATR-Ge, cm^{-1}) 3056 (C–H stretch), 1605 (C=O carbonyl stretch), 1621, 1594, 1570 (C–C aromatic stretch).

Elemental analysis: Calculated: 79.98% C; 5.37% H; 9.33% N. Found: 79.88% C; 5.47% H; 9.55% N.

4.2.2.9. 3-(3-fluoro-5-(trifluoromethyl)benzyl)-2-methylquinazolin-4(3H)-one

Code: GDM-2

Chemical structure:

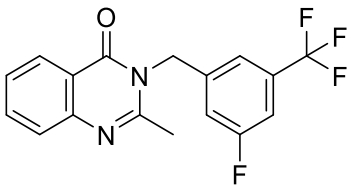

Chemical Formula: $C_{17}H_{12}F_4N_2O$

Molecular weight: 336.29 g/mol

Yield: 76%

Appearance: light beige solid

m.p.: 176–177 °C

R_f (Hexane/ EtOAc 2:1): 0.7

Log *P*: 4.02

^{1}H NMR: (600 MHz, $CDCl_3$) δ 8.32 – 8.28 (m, 1H), 7.94 – 7.87 (m, 1H), 7.81 – 7.74 (m, 1H), 7.71 – 7.67 (m, 1H), 7.64 – 7.44 (m, 1H), 7.43 – 7.28 (m, 1H), 6.84 – 6.80 (m, 1H), 5.82 (s, 2H, CH_2), 2.47 (s, 3H, CH_3).

^{13}C NMR: (151 MHz, DMSO-d_6) δ 162.06, 155.49, 147.65, 139.67, 135.13, 133.98, 131.26, 127.93, 127.21, 127.05, 126.96, 126.93, 125.50, 120.39, 46.56, 23.51.

Elemental analysis: Calculated: 60.72% C; 3.60% H; 8.33% N.

4.2.2.10. 3-(2,4-dichlorobenzyl)-2-methylquinazolin-4(3H)-one

Code: GDM-8

Chemical structure:

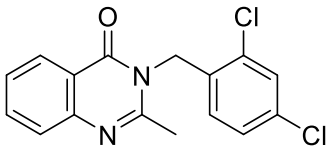

Chemical Formula: $C_{16}H_{12}C_{l2}N_2O$

Molecular weight: 319.19 g/mol

Yield: 46%

Appearance: white solid

m.p.: 172–173 °C

R_f (Hexanel/ EtOAc 2:1): 0.7

Log *P*: 4.06

^{1}H NMR: (600 MHz, $CDCl_3$) δ 8.32 – 8.25 (m, 1H), 7.80 – 7.74 (m, 1H), 7.66 (d, *J* = 8.2 Hz, 1H), 7.51 – 7.43 (m, 2H), 7.17 – 7.12 (m, 1H), 6.79 – 6.74 (m, 1H), 5.42 (s, 2H, CH_2), 2.49 (s, 3H, CH_3).

^{13}C NMR: (151 MHz, $CDCl_3$) δ 162.33, 154.21, 147.43, 134.80, 134.17, 133.24, 131.97, 129.74, 129.63, 127.87, 127.47, 127.21, 127.01, 120.23, 44.56, 23.14.

IR: (ATR-Ge, cm^{-1}) 3069 (C–H stretch), 1678 (C=O carbonyl stretch), 1595, 1566 (C–C aromatic stretch).

Elemental analysis: Calculated: 60.21% C; 3.79% H; 8.78% N. Found: 60.30% C; 3.70% H; 8.54% N.

4.2.2.11. (3,4-dichlorobenzyl)-2-methylquinazolin-4(3H)-one

Code: GDM-9

Chemical structure:

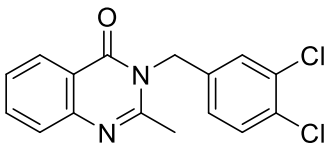

Chemical Formula: $C_{16}H_{12}Cl_2N_2O$

Molecular weight: 319.19 g/mol

Yield: 56%

Appearance: white solid

m.p.: 174–175 °C

R_f (Hexane/ EtOAc 2:1): 0.7

Log *P*: 4.06

^{1}H NMR: (600 MHz, $CDCl_3$) δ 8.25 – 8.20 (m, 1H), 7.73 – 7.67 (m, 1H), 7.61 – 7.56 (m, 1H), 7.47 – 7.39 (m, 1H), 7.33 (d, *J* = 8.3 Hz, 1H), 7.02 – 6.98 (m, 2H), 5.26 (s, 2H, CH_2), 2.10 (s, 3H, CH_3).

^{13}C NMR: (151 MHz, $CDCl_3$) δ 162.29, 154.01, 147.34, 136.30, 134.73, 133.24, 132.04, 131.00, 128.71, 127.13, 126.95, 126.85, 126.10, 120.28, 46.32, 23.47.

Elemental analysis: Calculated: 60.21% C; 3.79% H; 8.78% N. Found: 60.29% C; 3.71% H; 8.48% N.

4.3. Biological Assays

4.3.1. In Vitro Antibacterial Activity Evaluation

Microdilution broth method was used [29]. Antibacterial evaluation was performed against eight bacterial strains from the Czech Collection of Microorganisms (CCM, Brno, Czech Republic) (*Staphylococcus aureus* CCM 4223 (ATCC 29213), *Staphylococcus aureus* methicilin-resistant CCM 4750 (ATCC 43300), *Enterococcus faecalis* CCM 4224 (ATCC 29212), *Escherichia coli* CCM 3954 (ATCC 25922), *Pseudomonas aeruginosa* CCM 3955 (ATCC 27853)) or clinical isolates from the Department of Clinical Microbiology, University Hospital and Faculty of Medicine in Hradec Králové, Charles University in Prague, Czech Republic (*Staphylococcus epidermidis* 112-2016, *Klebsiella pneumoniae* 64-2016, *Serratia marcescens* 62-2016). All strains were subcultured on Mueller-Hinton agar (MHA) (Difco/Becton Dickinson, Detroit, MI, USA) at 35 ºC and maintained on the same medium at 4 ºC. The compounds were dissolved in DMSO, and the antibacterial activity was determined in cation adjusted Mueller-Hinton liquid broth (Difco/Becton Dickinson) buffered to pH 7.0. Controls consisted of medium and DMSO solely. The final concentration of DMSO in the test medium did not exceed 1% (*v/v*) of the total solution composition. The minimum inhibitory concentration (MIC) was determined after 24 and 48 h of static incubation at 35 ºC by visual inspection or using Alamar Blue dye. The standards were gentamicin and ciprofloxacin. All experiments were conducted in duplicate. For the results to be valid, the difference in MIC for one compound determined from two parallel measurements must not be greater than one step on the dilution scale. The methodology was followed as reported in one of our recent experimental works".[52]

4.3.2. In Vitro Activity Evaluation Against *Mycobacterium tuberculosis, Mycobacterium kansasii,* and *Mycobacterium avium*

Microdilution panel method. Tested strains *M. tuberculosis* H37Rv CNCTC My 331/88 (ATCC 27294), *M. kansasii* Hauduroy CNCTC My 235/80 (ATCC 12478), *M. avium* ssp. *Avium* Chester CNCTC My 80/72 (ATCC 15769) were obtained from the Czech National Collection of Type Cultures (CNCTC), National Institute of Public Health, Prague, Czech Republic. Middlebrook 7H9 broth (Sigma-Aldrich) enriched with 0.4% (*v/v*) of glycerol (Sigma-Aldrich) and 10% (*v/v*) of OADC supplement (oleic acid, albumin, dextrose, catalase; Himedia, Mumbai, India) of declared pH = 6.6. Tested compounds were dissolved and diluted in DMSO, mixed with broth (25 µL) of DMSO solution in 4.475 mL of broth and placed (100 µL) into microplate wells. Mycobacterial inocula were suspended in isotonic saline solution and the density was adjusted to 0.5–1.0 McFarland

scale. These suspensions were diluted by 10^{-1} and used to inoculate the testing wells, adding 100 µL of mycobacterial suspension per well. Final concentrations of the tested compounds in wells were 100, 50, 25, 12.5, 6.25, 3.13, and 1.56 µg/mL.

INH and PZA were used as positive controls (inhibition of growth). Negative control (mycobacterial growth control) consisted of broth plus DMSO. Plates were statically incubated in a dark, humid atmosphere at 37 ºC. After five days of incubation, 30 µL of Alamar Blue working solution (1:1 mixture of 0.1% resazurin sodium salt (aq. sol.) and 10% Tween 80) was added per well. Results were then determined after 24 h of incubation and interpreted according to Franzblau et al.[28]. The minimum inhibition concentration (MIC, µg/mL) was determined as the lowest concentration that prevented the blue to pink colour change as indicated by visual inspection. The experiments were conducted in duplicates. For the results to be valid, the difference in MIC for one compound determined from two parallel measurements must not be greater than one step on the dilution scale.

4.3.3. In Vitro Activity Evaluation Against *Mycobacterium smegmatis* and *Mycobacterium aurum*

The antimycobacterial assay was performed on fast-growing *M. smegmatis* DSM 43465 (ATCC 607) and *M. aurum* DSM 43999 (ATCC 23366) from the German Collection of Microorganisms and Cell Cultures (Braunschweig, Germany). The technique used for activity determination was microdilution broth panel method using 96-well microtitration plates. The culturing medium was Middlebrook 7H9 broth (Sigma-Aldrich) enriched with 0.4% of glycerol (Sigma-Aldrich) and 10% of Middlebrook OADC growth supplement (Himedia). Mycobacterial strains were cultured on Middlebrook 7H9 agar and suspensions were prepared in Middlebrook 7H9 broth. Final density was adjusted to value ranging from 0.5 to 1.0 according to McFarland scale and diluted in ratio 1:20 with broth. Tested compounds were dissolved in DMSO (Sigma-Aldrich), and then MB broth was added to obtain the concentration of 2000 µg/mL. Standards used for activity determination were INH, rifampicin (RIF) and ciprofloxacin (CPX) (Sigma-Aldrich). Final concentrations were reached by binary dilution and addition of mycobacterial suspension, and were set as 500, 250, 125, 62.5, 31.25, 15.625, 7.81, 3.91 µg/mL, except to standards rifampicin, where the final concentrations were 12.5, 6.25, 3.125, 1.56, 0.78, 0.39, 0.195, 0.098 µg/mL, and ciprofloxacin, where the final concentrations were 1, 0.5, 0.25, 0.125, 0.0625, 0.0313, 0.0156, 0.0078 µg/mL. The final concentration of DMSO did not exceed 2.5% (v/v) and did not affect the growth of *M. smegmatis* or *M. aurum*. Positive (broth, DMSO, bacteria) and negative (broth, DMSO) controls were included. Plates were sealed with polyester adhesive film and incubated in dark at 37 ºC

without agitation. The addition of 0.01% solution of resazurin sodium salt followed after 48 h of incubation for *M. smegmatis*, and after 72 h of incubation for *M. aurum*. Stain was prepared by dissolving resazurin sodium salt (Sigma-Aldrich) in deionised water to get 0.02% solution. Then 10% aqueous solution of Tween 80 (Sigma-Aldrich) was prepared. Equal volumes of both liquids were mixed and filtered through syringe membrane filter. Microtitration panels were then incubated for additional 2.5 h for determination of activity against *M. smegmatis*, and 4 h for *M. aurum*. Antimycobacterial activity was expressed as minimal inhibition concentration (MIC) and the value was read on the basis of stain colour change (blue colour—active compound; pink colour—inactive compound). MIC values for standards were in ranges 7.81–15.625 μg/mL for INH, 12.5–25 μg/mL for RIF, and 0.0625–0.125 μg/mL for CPX against *M. smegmatis*, 1.95–3.91 μg/mL for INH, 0.78–1.56 μg/mL for RIF, and 0.00781–0.01563 μg/mL for CPX against *M. aurum*, respectively. All experiments were conducted in duplicate. For the results to be valid, the difference in MIC for one compound determined from two parallel measurements must not be greater than one step on the dilution scale.

4.3.4. In Vitro Antifungal Activity Evaluation

Antifungal evaluation was performed using a microdilution broth method[30] against eight fungal strains from the Czech Collection of Microorganisms (CCM) (*Candida albicans* CCM 8320 (ATCC 24433), *C. krusei* CCM 8271 (ATCC 6258), *C. parapsilosis* CCM 8260 (ATCC 22019), *C. tropicalis* CCM 8264 (ATCC 750), *Aspergillus flavus* CCM 8363, *Absidia/Lichtheimia corymbifera* CCM 8077 and *Trichophyton interdigitale* CCM 8377 (ATCC 9533) or the American Type Collection Cultures (ATCC, *Mannasas*, VA, USA) (*Aspergillus fumigatus* ATCC 204305). Compounds were dissolved in DMSO and diluted in a twofold manner with RPMI 1640 medium, with glutamine and 2% glucose, buffered to pH 7.0 (3-morpholinopropane-1-sulfonic acid). The final concentration of DMSO in the tested medium did not exceed 2.5% (*v/v*) of the total solution composition. Static incubation was performed in the dark and in a humid atmosphere, at 35 ºC, for 24 and 48 h (72 and 120 h for *Trichophyton interdigitale,* respectively). Drug-free controls were included. MIC was inspected visually or making use of Alamar Blue staining. The standards were amphotericin B and fluconazole. All experiments were conducted in duplicate. For the results to be valid, the difference in MIC for one compound determined from two parallel measurements must not be greater than one step on the dilution scale.

5. RESULTS AND DISCUSSION

5.1.1. Chemistry

The final products were purified using flash chromatography, using ethyl acetate in hexane as eluent. They were isolated as light-colored, solid compounds, in yields ranging from 23–88% of chromatographically pure products. Compounds with more lipophilic substituents tend to have higher yields compared to more hydrophilic ones (refer to Table 3).

We searched for final compounds in the freely available tool ChemSpider provided by the Royal Society of Chemistry (RSC) (www.chemspider.com). The results of the search are summarized in Table 4 below. None of the final compounds were previously evaluated for biological activities.

Table 4. Results of literature search in ChemSpider (www.chemspider.com) for title compounds.

Code	ChemSpider ID	Literature (RSC journals/PubMed)
GDM-12	NA	NA
GDM-15	6784121	NA
GDM-14	31019715	NA
GDM-4	6784297	NA
GDM-13	6784416	NA
GDM-10	6782760	NA
GDM-7	NA	NA
GDM-N	NA	NA
GDM-2	NA	NA
GDM-8	6782738	NA
GDM-9	6782752	NA

Note: NA = not available.

5.1.2. Predicted pharmacokinetics, drug-likeness, and medicinal chemistry features

We used the free web tool SwissADME to evaluate pharmacokinetics, drug-likeness and medicinal chemistry friendliness of our title compounds.[53] We selected the most relevant properties and presented them in tables 5–7 below. Most importantly, all of the title compounds satisfied Lipinski rule of 5 and passed Pan-Assay Interference Structure filter (PAINS). Additionally, all compounds confer the parameters of Leadlikeness,[54–56] with the exception of compounds GDM-N, GMD-8, and GDM-9, all of which have XLOGP3 above 3.5.

Table 5. The physicochemical properties of final compounds predicted using SwissADME tool.

Code	Num. heavy atoms	Num. rotatable bonds	Num. H-bond acceptors	Num. H-bond donors	Molar Refractivity	Topological Polar Surface Area (TPSA)
GDM12	23	4	4	0	89.70	53.35 Å²
GDM15	21	3	3	0	83.21	44.12 Å²
GDM14	21	3	3	0	83.21	44.12 Å²
GDM4	20	2	3	0	76.68	34.89 Å²
GDM13	20	2	2	0	81.68	34.89 Å²
GDM10	20	2	2	0	81.73	34.89 Å²
GDM7	23	3	5	0	81.72	34.89 Å²
GDMN	23	2	2	0	94.22	34.89 Å²
GDM2	24	3	6	0	81.68	34.89 Å²
GDM8	21	2	2	0	86.74	34.89 Å²
GDM9	21	2	2	0	86.74	34.89 Å²

Table 6. The Pharmacokinetics properties of final compounds predicted using SwissADME tool.

Code	GI absorption	BBB permeant	P-gp substrate	CYP1A2 inhibitor	CYP3A4 inhibitor	Log Kp (skin permeation) in cm/s
GDM12	High	Yes	No	Yes	yes	-6.55 cm/s
GDM15	High	Yes	No	Yes	yes	-6.35 cm/s
GDM14	High	Yes	No	Yes	yes	-6.35 cm/s
GDM4	High	Yes	No	Yes	No	-6.18 cm/s
GDM13	High	Yes	No	Yes	No	-5.97 cm/s
GDM10	High	Yes	No	Yes	No	-5.91 cm/s
GDM7	High	Yes	No	Yes	No	-5.93 cm/s
GDMN	High	Yes	No	Yes	Yes	-5.56 cm/s
GDM2	High	Yes	No	Yes	No	-5.97 cm/s
GDM8	High	Yes	No	Yes	No	-5.68 cm/s
GDM9	High	Yes	No	Yes	No	-5.68 cm/s

Table 7. The druglikeness and medicinal chemistry properties of final compounds predicted using SwissADME tool.

Code	Lipinski	Bioavailability Score	Pan Assay Interference Structure (PAINS)	Leadlikeness
GDM12	Yes; 0 violations	0.55	0 alert	yes
GDM15	Yes; 0 violations	0.55	0 alert	yes
GDM14	Yes; 0 violations	0.55	0 alert	yes
GDM4	Yes; 0 violations	0.55	0 alert	yes
GDM13	Yes; 0 violations	0.55	0 alert	yes
GDM10	Yes; 0 violations	0.55	0 alert	yes
GDM7	Yes; 0 violations	0.55	0 alert	yes
GDMN	Yes; 0 violations	0.55	0 alert	No; 1 violation: XLOGP3>3.5
GDM2	Yes; 0 violations	0.55	0 alert	yes

GDM8	Yes; 0 violations	0.55	0 alert	No; 1 violation: XLOGP3>3.5
GDM9	Yes; 0 violations	0.55	0 alert	No; 1 violation: XLOGP3>3.5

5.1.3. Antibacterial activity

In a microdilution in vitro assay, the final compounds were screened against four Gram-positive [*Staphylococcus aureus* (*SA*), methicillin-resistant *Staphylococcus aureus* (MRSA), *Staphylococcus epidermidis* (SE), *Enterococcus faecalis* (EF)] and four Gram-negative [*Escherichia coli* (EC), *Klebsiella pneumoniae* (KP), *Serratia marcescens* (SM), *Pseudomonas aeruginosa* (PA)] bacterial strains of clinical importance. Antibacterial activity is expressed as MIC in µM. The discussed MIC values were read after 24 h and 48 h of incubation. All MIC values obtained from the two time points were indifferent for each pathogen. It was not possible to screen compounds GDMN, GDM8, and GDM9 due to their low solubility and precipitation in testing media. Besides that, no significant antibacterial activity was detected for any of the tested compounds. Compounds GDM15 (24 h MIC/IC_{95} = 500 µM), GDM14 (24 h MIC/IC_{95} = 62.5 µM), GDM10 (24 h MIC/IC_{95} = 250 µM), GDM7 (24 h MIC/IC_{95} = 250 µM), and GDM2 (24 h MIC/IC_{95} = 125 µM) exerted mild activity against *SE* strain.

Table 8. Antibacterial activities of final compounds expressed as MIC/IC_{95} in µM.

		MIC/IC_{95} (µM)							
		GDM12	**GDM15**	**GDM14**	**GDM4**	**GDM13**	**GDM10**	**GDM7**	**GDM2**
SA	24h	>500	**500**	>125	>500	>500	>500	>500	>125
	48h	>500	**500**	>125	>500	>500	>500	>500	>125
MRSA	24h	>500	>500	>125	>500	>500	>500	>500	>125
	48h	>500	>500	>125	>500	>500	>500	>500	>125
SE	24h	>500	**500**	**62.5**	>500	>500	**250**	**250**	**125**
	48h	>500	**500**	**62.5**	>500	>500	**500**	**250**	**125**
EF	24h	>500	>500	>125	>500	>500	>500	**500**	>125
	48h	>500	>500	>125	>500	>500	>500	>500	>125
EC	24h	>500	>500	>125	>500	>500	>500	>500	>125
	48h	>500	>500	>125	>500	>500	>500	>500	>125
KP	24h	>500	>500	>125	>500	>500	>500	>500	>125
	48h	>500	>500	>125	>500	>500	>500	>500	>125
ACI	24h	>500	>500	>125	>500	>500	>500	>500	>125
	48h	>500	>500	>125	>500	>500	>500	>500	>125
PA	24h	>500	>500	>125	>500	>500	>500	>500	>125
	48h	>500	>500	>125	>500	>500	>500	>500	>125

Note: Bacterial strains listed in the table are as follows:
SA = *Staphylococcus aureus* subsp. *aureus* ATCC 29213, CCM 4223
MRSA = *Staphylococcus aureus* subsp.aureus ATCC 43300, CCM 4750
SE = *Staphylococcus epidermidis* ATCC 12228, CCM 4418
EF = *Enterococcus faecalis* ATCC 29212, CCM 4224
EC = *Escherichia coli* ATCC 25922, CCM 3954
KP = *Klebsiella pneumoniae* ATCC 10031, CCM 4415
ACI = *Acinetobacter baumannii* ATCC 19606, DSM 30007
PA = *Pseudomonas aeruginosa* ATCC 27853, CCM 3955

5.1.4. Antimycobacterial Activity

As complementary testing, final compounds were evaluated for their antimycobacterial effects against the pathogenic, slow-growing strains *Mycobacterium tuberculosis* H37Rv (*Mtb*), *M. kansasii*, and *M. avium*. It is reported in the literature that the MIC values against MtbH37Ra (avirulent strain) are at least qualitatively equivalent to MIC values against the virulent strain of Mtb H37Rv [12]. Therefore, this avirulent strain Mtb H37 Ra can be treated as a surrogate for the highly pathogenic Mtb H37Rv. *M. smegmatis* and *M. aurum* on the other hand are fast-growing mycobacteria that cause infection only in patients with weak immune systems. At the same time, these two mycobacterial species are surrogate organisms, having a cell wall structure and resistance profile very close to Mtb H37Rv.

Antimycobacterial activity is expressed as minimal inhibitory concentration (MIC) in μg/mL and summarized in Table 9. Compounds are ordered in the table in ascending order depending on their lipophilicity (log *P* value). Activity cutoff is set to be 62.5 μg/mL, below of which activity is considered to be significant. According to Table 9, we can conclude that compounds exerted significant activity against *M. kansasii* strain specifically. An exception to this is compound GDM 10 (R = 3-Cl) which, in addition to being the most active compound against *M. kansasii* (MIC = 7.81 μg/mL), also exerted antimycobacterial activity against *Mtb* H37Ra (MIC = 31.25 μg/mL) and *M. avium* (MIC = 31.25 μg/mL), making it the most broad-spectrum compound and hence most promising. Worth to mention that *M. kansasii* is one of the most common type of nontuberculous mycobacteria (*NTM*) that can cause lung disease similarly as tuberculosis.[57] Despite that the infections caused by *M. kansasii* are less common in comparison to typical *TB* caused by *Mtb*; the incidence of *NTM* disease is rising globally. According to a recent analysis of the prevalence of *M. kansasii* in clinical and environmental isolates by Narimisa et al., an increase in the prevalence of *M. kansasii* over the years has been reported.[57] In general, infections caused by *M. kansasii* are considered less virulent than TB caused by *Mtb*, but immunocompromised individuals may lead to the development of severe disease.[58] Treatment of *M. kansasii* infections could be complicated due to the requirement of long-term administration. The first choice therapy recommended by IDSA-ATS guidelines for M. kansasii is rifampin, ethambutol, isoniazid and pyridoxine. The optimum duration of therapy is at least 12 months or even more to have culture-negative results for 12 months on therapy of antimycobacterial agents, which is accompanied by side effects and, consequently, non-adherence of patients.[59,60]

Table 9. Prepared compounds with their calculated lipophilicity (log *P*, ChemDraw v22.0.), antimycobacterial activity expressed as minimum inhibitory concentration (MIC) in µg/mL.

Cmpd.	CODE	R	log*P*	Antimycobacterial Activity MIC in µg/mL					
				***Mtb* H37Rv**	***Mtb* H37Ra**	***M. kansasii***	***M. avium***	***M. smeg***	***M. aurum***
1	**GDM12**	2,4-diOCH_3	2.69	>100	≥500	15.625	≥500	≥500	≥500
2	**GDM15**	3-OCH_3	2.82	100	62.5	15.625	62.5	250	125
3	**GDM14**	4-OCH_3	2.82	>100	≥250	15.625	≥250	≥250	≥250
4	**GDM4**	3-F	3.1	100	250	15.625	125	250	500
5	**GDM13**	2-CH_3	3.43	>100	≥500	15.625	≥500	≥500	≥500
6	**GDM10**	3-Cl	3.5	50	31.25	7.81	31.25	62.5	62.5
7	**GDM7**	4-CF_3	3.86	>100	62.5	62.5	125	250	125
8	**GDMN**	naphthyl	3.94	>100	≥250	15.625	62.5	≥500	62.5
9	**GDM2**	3-F, 5-CF_3	4.02	>100	125	7.81	62.5	≥500	62.5
10	**GDM8**	2,4-diCl	4.06	>100	≥250	15.625	≥250	≥250	≥250
11	**GDM9**	3,4-diCl	4.06	>100	≥250	15.625	≥250	≥250	≥250
INH				0.2	0.25	6.25	1000	15.625	3.91
RIF					0.0015625	0.025	0.125	12.5	0.39
CIP					0.25	0.25	1.56	0.125	0.015625

5.1.5. Antifungal activity

In a microdilution in vitro assay, the final compounds were screened against eight fungal strains [*Candida albicans* (CA), *Candida krusei* (CK), *Candida parapsilosis* (CP), *Candida tropicalis* (CT), *Aspergillus fumigatus* (AF), *Aspergillus flavus* (AFla), *Absidia corymbifera* (AC), *Trichophyton interdigitale* (TI)] of clinical importance. Antifungal activity is expressed as MIC in µM. The discussed MIC values were read after 24 h and 48 h of incubation, except for TI for which the MIC values were measured after 72 h and 120 h of incubation time. All MIC values obtained from the two time points were indifferent for each pathogen. No significant antifungal activity was detected for any of the tested compounds.

Table 10. Antibacterial activities of final compounds expressed as MIC/IC_{95} in µM.

		MIC/IC_{95} (µM)							
		GDM12	**GDM15**	**GDM14**	**GDM4**	**GDM13**	**GDM10**	**GDM7**	**GDM2**
CA	24h	>500	>500	>125	>500	>500	>500	>500	>125
	48h	>500	>500	>125	>500	>500	>500	>500	>125
CK	24h	>500	>500	>125	>500	>500	>500	>500	>125
	48h	>500	>500	>125	>500	>500	>500	>500	>125
CP	24h	>500	>500	>125	>500	>500	>500	>500	>125
	48h	>500	>500	>125	>500	>500	>500	>500	>125
CT	24h	>500	>500	>125	>500	>500	>500	>500	>125
	48h	>500	>500	>125	>500	>500	>500	>500	>125
AF	24h	>500	>500	>125	>500	>500	>500	>500	>125
	48h	>500	>500	>125	>500	>500	>500	>500	>125
AFla	24h	>500	>500	>125	>500	>500	>500	>500	>125
	48h	>500	>500	>125	>500	>500	>500	>500	>125
AC	24h	>500	>500	>125	>500	>500	>500	>500	>125
	48h	>500	>500	>125	>500	>500	>500	>500	>125
TI	5dnů	>500	>500	>125	>500	>500	**500**	>500	>125
	7dnů	>500	>500	>125	>500	>500	**500**	>500	>125

Note: Fungal strains listed in the table are as follows
CA = *Candida albicans* ATCC 24433, CCM 8320
CK = *Candida krusei* ATCC 6258, CCM 8271
CP = *Candida parapsilosis* ATCC 22019, CCM 8260
CT = *Candida tropicalis* ATCC 750, CCM 8264
AF = *Aspergillus fumigatus* ATCC 204305
AFla = *Aspergillus flavus* CCM 8363
AC = *Absidia corymbifera* CCM 8077
TI = *Trichophyton interdigitale* ATCC 9533, CCM 8377

6. CONCLUSIONS

To conclude, the work reported in this diploma thesis is part of a broader series originally designed as potential biologically active compounds against the troublesome bacteria, S*taphylococcus aureus (SA*). The chemical structure of the original parent compound was designed based on what is reported in the literature for antistaphylococcal quinazolinones and in silico docking studies performed by other colleagues in our research group. The intended structures were proposed to target penicillin binding protein in *SA*. Eleven final compounds with different lipophilicity with log *P* values ranging between 2.69 and 4.06 were prepared by reacting the lactone intermediate, benzoxazinone, with different benzyl amines. Closely related series by my colleagues have a chlorine atom at position 7 of the quinazolinone ring, while another series has a different bridge than the methylene linker used in this diploma thesis.

Despite the original design as antistaphylococcal active agents, none of the final compounds exerted significant antistaphylococcal activity. As complementary testing, final compounds were screened against a panel of pathogens, including some gram-positive bacteria, gram-negative bacteria, mycobacteria, and fungi. Among these, most of the prepared compounds exerted selective, potent, antimycobacterial activity against *M. kansasii* that is worth further exploration. GDM-10 (R = 3-Cl) was among the most active compounds against *M. kansasii* (MIC = 7.81 μg/mL), with extended spectrum of activity to include *Mtb* H37Ra (MIC = 31.25 μg/mL) and *M. avium* (MIC = 31.25 μg/mL), making it the most promising compound. Our results suggest shifting the focus of such design toward mycobacteria rather than *SA*. Future work shall investigate whether mycobacteria penicillin binding protein is the target of the active compounds. We used the online, freely available tool ChemSpider provided by the Royal Society of Chemistry (RSC) (www.chemspider.com) to check the originality of our final compounds. Seven compounds had ChemSpider identifier number, namely GDM-15, GDM-14, GDM-4, GDM-13, GDM-10, GDM-8, and GDM-9, yet none of the title compounds were part of a published work when searched in RSC journals or PubMed database, according to ChemSpider tool.

7. ABSTRAKT (CZECH)

Univerzita Karlova, Farmaceutická fakulta v Hradci Králové, Katedra farmaceutické chemie a farmaceutické analýzy

Řešitel: Asal Askari
Vedoucí diplomové práce: doc. PharmDr. Jan Zitko, Ph.D.
Konzultant: Ghada Bouz, Ph.D.
Název diplomové práce: Návrh, syntéza a hodnocení heterocyklických sloučenin s potenciální antimikrobní aktivitou V

Staphylococcus aureus (*SA*) je jednou z nejčastějších příčin život ohrožujících infekcí. Jedním ze způsobů, jak kontrolovat infekčnost *SA*, je vývoj inovativních látek, nejlépe s novým mechanismem účinku, které jsou účinné jak proti kmenům citlivým na léky, tak proti kmenům lékově rezistentním. Chinazolon slouží jako základní kostra pro mnoho různých biologicky aktivních sloučenin. Antistafylokokové chinazolony (AQs) mají v literatuře popsané vztahy mezi strukturou a aktivitou. Penicilin vázající protein (PBP), DNA topoizomeráza a laktátdehydrogenáza jsou některé z molekulárních cílů pro AQs.

S využitím in silico molekulového dokování jsme spojili naše rozsáhlé znalosti antibakteriálních léčiv s tím, co bylo popsáno v literatuře, abychom vytvořili nové, potenciálně aktivní AQs zaměřené na PBP. Výsledkem bylo, že jsme připravili 11 finálních sloučenin s lipofilitou v rozmezí 2,69 až 4,06 reakcí laktonového meziproduktu, benzoxazinonu, s různými benzylaminy. Navzdory původnímu návrhu jako antistafylokokové účinné látky nevykazovala žádná z finálních sloučenin významnou antistafylokokovou aktivitu. Jako doplňkové testování byly finální sloučeniny testovány proti panelu patogenů, včetně některých grampozitivních bakterií, gramnegativních bakterií, mykobakterií a hub/plísní. Sloučenina GDM-10 (R = 3-Cl) patřila mezi nejaktivnější sloučeniny proti *M. kansasii* (MIC = 7,81 µg/ml), s rozšířeným spektrem aktivity o Mtb H37Ra MIC = 31,25 µg/ml) a *M. avium* (MIC = 31,25 µg/ml), což z ní činí nejslibnější sloučeninu. Naše výsledky naznačují, že se zaměření takto navržených sloučenin přesouvá spíše na mykobakterie než na SA. Budoucí práce bude zkoumat, zda je cílem účinných látek mykobakteriální protein vázající penicilin (PBP).

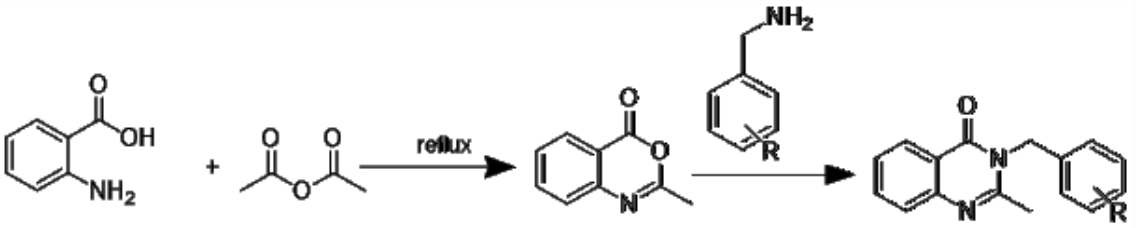

Obrázek 1. Obecný postup a struktury finálních sloučenin připravených v této diplomové práci. R = 2,4-diMeO; 3-MeO; 4-MeO; 3-F; 2-Me; 3-Cl; 4-CF_3; 2,4-diCl; 3,4-diCl atd.

8. ABSTRACT (ENGLISH)

Charles University, Faculty of Pharmacy in Hradec Králové. Department of Pharmaceutical Chemistry and Pharmaceutical Analysis

Author: Asal Askari
Supervisor: Assoc. Prof. PharmDr. Jan Zitko, Ph.D.
Consultant: Ghada Bouz, Ph.D.
Title of diploma thesis: Design, Synthesis, and Evaluation of Heterocyclic Compounds with Potential Antimicrobial Activity V

Staphylococcus aureus (*SA*) is one of the most common causes of life-threatening infections. One of the ways to control *SA* infectious is the development of innovative agents, preferably with novel mechanism of action, that are efficient against both drug-sensitive and drug-resistant strains. Quinazolone serves as an essential backbone for many different biologically active compounds. Antistaphylococcal quinazolones (AQs) have established structure activity relationships in the literature. Penicillin binding protein (PBP), DNA topoisomerase, and lactate dehydrogenase are few of the molecular targets for AQs.

With the use of *in silico* docking, we coupled our extensive antibacterial knowledge with what has been described in the literature to create novel, potentially active AQs targeting PBP. As result, we prepared 11 final compounds with ranging lipophilicity between 2.69 and 4.06 by reacting the lactone intermediate, benzoxazinone, with different benzyl amines. Despite the original design as antistaphylococcal active agents, none of the final compounds exerted significant antistaphylococcal activity. As complementary testing, final compounds were screened against a panel of pathogens, including some gram-positive bacteria, gram-negative bacteria, mycobacteria, and fungi. GDM-10 (R = 3-Cl) was among the most active compounds against *M. kansasii* (MIC = 7.81 µg/mL), with extended spectrum of activity to include *Mtb* H37Ra (MIC = 31.25 µg/mL) and *M. avium* (MIC = 31.25 µg/mL), making it the most promising compound. Our results suggest shifting the focus of such designed compounds toward mycobacteria rather than *SA.* Future work shall investigate whether mycobacteria penicillin binding protein is the target of active compounds.

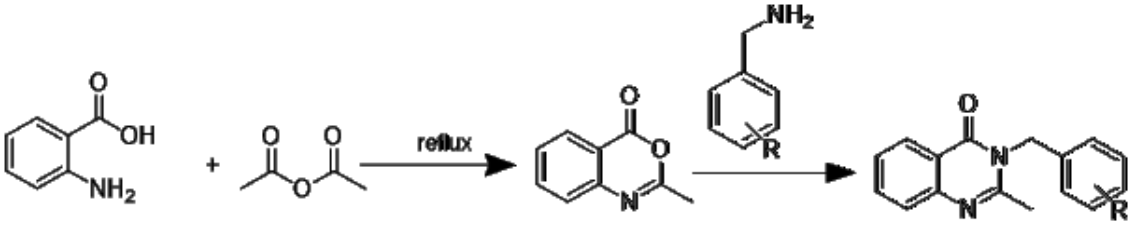

Figure 1. The general procedure and structures of final compounds prepared in this diploma.
R= 2,4-diMeO; 3-MeO; 4-MeO; 3-F; 2-Me; 3-Cl; 4-CF_3; 2,4-diCl; 3,4-diCl; etc

9. REFERENCES

[1] W.C. Reygaert, An overview of the antimicrobial resistance mechanisms of bacteria, AIMS Microbiol. 4 (2018) 482–501. https://doi.org/10.3934/microbiol.2018.3.482.

[2] J.M. Munita, C.A. Arias, Mechanisms of Antibiotic Resistance, Microbiol. Spectr. 4 (2016) 10.1128/microbiolspec.VMBF-0016–2015. https://doi.org/10.1128/microbiolspec.VMBF-0016-2015.

[3] E. Jafari, M.R. Khajouei, F. Hassanzadeh, G.H. Hakimelahi, G.A. Khodarahmi, Quinazolinone and quinazoline derivatives: recent structures with potent antimicrobial and cytotoxic activities, Res. Pharm. Sci. 11 (2016) 1–14.

[4] S.Y.C. Tong, J.S. Davis, E. Eichenberger, T.L. Holland, V.G. Fowler, Staphylococcus aureus Infections: Epidemiology, Pathophysiology, Clinical Manifestations, and Management, Clin. Microbiol. Rev. 28 (2015) 603–661. https://doi.org/10.1128/CMR.00134-14.

[5] B.P. Howden, S.G. Giulieri, T. Wong Fok Lung, S.L. Baines, L.K. Sharkey, J.Y.H. Lee, A. Hachani, I.R. Monk, T.P. Stinear, Staphylococcus aureus host interactions and adaptation, Nat. Rev. Microbiol. 21 (2023) 380–395. https://doi.org/10.1038/s41579-023-00852-y.

[6] E.F. Kong, J.K. Johnson, M.A. Jabra-Rizk, Community-Associated Methicillin-Resistant Staphylococcus aureus: An Enemy amidst Us, PLOS Pathog. 12 (2016) e1005837. https://doi.org/10.1371/journal.ppat.1005837.

[7] D.L. Boger, Vancomycin, teicoplanin, and ramoplanin: synthetic and mechanistic studies, Med. Res. Rev. 21 (2001) 356–381. https://doi.org/10.1002/med.1014.

[8] K. Bush, P.A. Bradford, β-Lactams and β-Lactamase Inhibitors: An Overview, Cold Spring Harb. Perspect. Med. 6 (2016) a025247. https://doi.org/10.1101/cshperspect.a025247.

[9] C. Roger, J.A. Roberts, L. Muller, Clinical Pharmacokinetics and Pharmacodynamics of Oxazolidinones, Clin. Pharmacokinet. 57 (2018) 559–575. https://doi.org/10.1007/s40262-017-0601-x.

[10] M. Heidary, A.D. Khosravi, S. Khoshnood, M.J. Nasiri, S. Soleimani, M. Goudarzi, Daptomycin, J. Antimicrob. Chemother. 73 (2018) 1–11. https://doi.org/10.1093/jac/dkx349.

[11] R.F. Eyler, K. Shvets, Clinical Pharmacology of Antibiotics, Clin. J. Am. Soc. Nephrol. CJASN 14 (2019) 1080–1090. https://doi.org/10.2215/CJN.08140718.

[12] P.H. Patel, M.F. Hashmi, Macrolides, in: StatPearls, StatPearls Publishing, Treasure Island (FL), 2024. http://www.ncbi.nlm.nih.gov/books/NBK551495/ (accessed May 12, 2024).

[13] M. Block, D.L. Blanchard, Aminoglycosides, in: StatPearls, StatPearls Publishing, Treasure Island (FL), 2024. http://www.ncbi.nlm.nih.gov/books/NBK541105/ (accessed May 12, 2024).

[14] A. Fàbrega, S. Madurga, E. Giralt, J. Vila, Mechanism of action of and resistance to quinolones, Microb. Biotechnol. 2 (2009) 40–61. https://doi.org/10.1111/j.1751-7915.2008.00063.x.

[15] P.B. Murphy, K.G. Bistas, J.K. Le, Clindamycin, in: StatPearls, StatPearls Publishing, Treasure Island (FL), 2024. http://www.ncbi.nlm.nih.gov/books/NBK519574/ (accessed May 12, 2024).

[16] M.A. Parenti, S.M. Hatfield, J.J. Leyden, Mupirocin: a topical antibiotic with a unique structure and mechanism of action, Clin. Pharm. 6 (1987) 761–770.

[17] T. Li, Z. Wang, J. Guo, C. de la Fuente-Nunez, J. Wang, B. Han, H. Tao, J. Liu, X. Wang, Bacterial resistance to antibacterial agents: Mechanisms, control strategies, and implications for global health, Sci. Total Environ. 860 (2023) 160461. https://doi.org/10.1016/j.scitotenv.2022.160461.

[18] D. Tălăpan, A.-M. Sandu, A. Rafila, Antimicrobial Resistance of Staphylococcus aureus Isolated between 2017 and 2022 from Infections at a Tertiary Care Hospital in Romania, Antibiot. Basel Switz. 12 (2023) 974. https://doi.org/10.3390/antibiotics12060974.

[19] G. Zhou, Q.-S. Shi, X.-M. Huang, X.-B. Xie, The Three Bacterial Lines of Defense against Antimicrobial Agents, Int. J. Mol. Sci. 16 (2015) 21711–21733. https://doi.org/10.3390/ijms160921711.
[20] Md.A. Salam, Md.Y. Al-Amin, M.T. Salam, J.S. Pawar, N. Akhter, A.A. Rabaan, M.A.A. Alqumber, Antimicrobial Resistance: A Growing Serious Threat for Global Public Health, Healthcare 11 (2023) 1946. https://doi.org/10.3390/healthcare11131946.
[21] A.C. Rios, C.G. Moutinho, F.C. Pinto, F.S. Del Fiol, A. Jozala, M.V. Chaud, M.M.D.C. Vila, J.A. Teixeira, V.M. Balcão, Alternatives to overcoming bacterial resistances: *State-of-the-art*, Microbiol. Res. 191 (2016) 51–80. https://doi.org/10.1016/j.micres.2016.04.008.
[22] A. Pantosti, A. Sanchini, M. Monaco, Mechanisms of antibiotic resistance in Staphylococcus aureus, Future Microbiol. 2 (2007) 323–334. https://doi.org/10.2217/17460913.2.3.323.
[23] T.M. Uddin, A.J. Chakraborty, A. Khusro, B.R.M. Zidan, S. Mitra, T.B. Emran, K. Dhama, Md.K.H. Ripon, M. Gajdács, M.U.K. Sahibzada, Md.J. Hossain, N. Koirala, Antibiotic resistance in microbes: History, mechanisms, therapeutic strategies and future prospects, J. Infect. Public Health 14 (2021) 1750–1766. https://doi.org/10.1016/j.jiph.2021.10.020.
[24] M.N. Alekshun, S.B. Levy, Molecular Mechanisms of Antibacterial Multidrug Resistance, Cell 128 (2007) 1037–1050. https://doi.org/10.1016/j.cell.2007.03.004.
[25] A.B. Eyoh, M. Toukam, J. Atashili, C. Fokunang, H. Gonsu, E.E. Lyonga, H. Mandi, G. Ikomey, B. Mukwele, M. Mesembe, M.C.O. Assoumou, Relationship between multiple drug resistance and biofilm formation in Staphylococcus aureus isolated from medical and non-medical personnel in Yaounde, Cameroon, Pan Afr. Med. J. 17 (2014) 186. https://doi.org/10.11604/pamj.2014.17.186.2363.
[26] F.D. Lowy, Antimicrobial resistance: the example of Staphylococcus aureus, J. Clin. Invest. 111 (2003) 1265–1273. https://doi.org/10.1172/JCI200318535.
[27] Y. Guo, G. Song, M. Sun, J. Wang, Y. Wang, Prevalence and Therapies of Antibiotic-Resistance in Staphylococcus aureus, Front. Cell. Infect. Microbiol. 10 (2020) 107. https://doi.org/10.3389/fcimb.2020.00107.
[28] M. Lobanovska, G. Pilla, Penicillin's Discovery and Antibiotic Resistance: Lessons for the Future?, Yale J. Biol. Med. 90 (2017) 135–145.
[29] H. Lade, J.-S. Kim, Molecular Determinants of β-Lactam Resistance in Methicillin-Resistant Staphylococcus aureus (MRSA): An Updated Review, Antibiotics 12 (2023) 1362. https://doi.org/10.3390/antibiotics12091362.
[30] J.M. Boyce, B. Cookson, K. Christiansen, S. Hori, J. Vuopio-Varkila, S. Kocagöz, A.Y. Öztop, C.M. Vandenbroucke-Grauls, S. Harbarth, D. Pittet, Meticillin-resistant Staphylococcus aureus, Lancet Infect. Dis. 5 (2005) 653–663. https://doi.org/10.1016/S1473-3099(05)70243-7.
[31] R.R. Gurung, P. Maharjan, G.G. Chhetri, Antibiotic resistance pattern of Staphylococcus aureus with reference to MRSA isolates from pediatric patients, Future Sci. OA 6 (n.d.) FSO464. https://doi.org/10.2144/fsoa-2019-0122.
[32] E.E. Udo, Community-Acquired Methicillin-Resistant Staphylococcus aureus: The New Face of an Old Foe?, Med. Princ. Pract. 22 (2013) 20–29. https://doi.org/10.1159/000354201.
[33] T.J. Foster, Antibiotic resistance in Staphylococcus aureus. Current status and future prospects, FEMS Microbiol. Rev. 41 (2017) 430–449. https://doi.org/10.1093/femsre/fux007.
[34] A. Bitrus, M. Olabode, M. Abbas, M. Dauda Goni, Staphylococcus aureus: A Review of Antimicrobial Resistance Mechanism, Vet. Sci. Res. Rev. 4 (2018). https://doi.org/10.17582/journal.vsrr/2018/4.2.43.54.
[35] B. Mlynarczyk-Bonikowska, C. Kowalewski, A. Krolak-Ulinska, W. Marusza, Molecular Mechanisms of Drug Resistance in Staphylococcus aureus, Int. J. Mol. Sci. 23 (2022) 8088. https://doi.org/10.3390/ijms23158088.

[36] S.M. Swaney, H. Aoki, M.C. Ganoza, D.L. Shinabarger, The Oxazolidinone Linezolid Inhibits Initiation of Protein Synthesis in Bacteria, Antimicrob. Agents Chemother. 42 (1998) 3251–3255.
[37] Z. Shi, J. Zhang, L. Tian, L. Xin, C. Liang, X. Ren, M. Li, A Comprehensive Overview of the Antibiotics Approved in the Last Two Decades: Retrospects and Prospects, Molecules 28 (2023) 1762. https://doi.org/10.3390/molecules28041762.
[38] Y. Doi, J. Wachino, Y. Arakawa, Aminoglycoside Resistance, Infect. Dis. Clin. North Am. 30 (2016) 523–537. https://doi.org/10.1016/j.idc.2016.02.011.
[39] K.M. Krause, A.W. Serio, T.R. Kane, L.E. Connolly, Aminoglycosides: An Overview, Cold Spring Harb. Perspect. Med. 6 (2016) a027029. https://doi.org/10.1101/cshperspect.a027029.
[40] VISA/VRSA in Healthcare Settings | HAI | CDC, (2019). https://www.cdc.gov/hai/organisms/visa_vrsa/visa_vrsa.html (accessed May 13, 2024).
[41] J.M. Conly, B.L. Johnston, VISA, hetero-VISA and VRSA: The end of the vancomycin era?, Can. J. Infect. Dis. 13 (2002) 282–284.
[42] S. Gardete, A. Tomasz, Mechanisms of vancomycin resistance in Staphylococcus aureus, J. Clin. Invest. 124 (2014) 2836–2840. https://doi.org/10.1172/JCI68834.
[43] WHO publishes list of bacteria for which new antibiotics are urgently needed, (n.d.). https://www.who.int/news/item/27-02-2017-who-publishes-list-of-bacteria-for-which-new-antibiotics-are-urgently-needed (accessed May 13, 2024).
[44] D. Nawrot, W. Ambrożkiewicz-Mosler, M. Doležal, G. Bouz, Antistaphylococcal discovery pipeline; where are we now?, Eur. J. Med. Chem. 266 (2024) 116077. https://doi.org/10.1016/j.ejmech.2023.116077.
[45] B. Kumar Tiwary, K. Pradhan, A. Kumar Nanda, R. Chakraborty, Implication of Quinazoline-4(3H)-ones in Medicinal Chemistry: A Brief Review, in: J. Chem. Biol. Ther., 2016. https://doi.org/10.4172/2572-0406.1000104.
[46] R. Bansal, A. Malhotra, Therapeutic progression of quinazolines as targeted chemotherapeutic agents, Eur. J. Med. Chem. 211 (2021) 113016. https://doi.org/10.1016/j.ejmech.2020.113016.
[47] P. Theivendren, P. Kumar, Quinazoline Marketed drugs – A Review, Res Pharm 1 (2011) 1–21.
[48] Y.N. Mabkhot, M.S. Al-Har, A. Barakat, F.D. Aldawsari, A. Aldalbahi, Z. Ul-Haq, Synthesis, Anti-microbial and Molecular Docking Studies of Quinazolin-4(3H)-one Derivatives, Molecules 19 (2014) 8725–8739. https://doi.org/10.3390/molecules19078725.
[49] P. Patel, H. Joshi, U. Shah, M. Bapna, B. Patel, New Generation of Quinazolinone Derivatives as Potent Antimicrobial Agents, Asian Pac. J. Health Sci. 8 (2021). https://doi.org/10.21276/apjhs.2021.8.2.12.
[50] J. Janardhanan, R. Bouley, S. Martínez-Caballero, Z. Peng, M. Batuecas-Mordillo, J.E. Meisel, D. Ding, V.A. Schroeder, W.R. Wolter, K.V. Mahasenan, J.A. Hermoso, S. Mobashery, M. Chang, The Quinazolinone Allosteric Inhibitor of PBP 2a Synergizes with Piperacillin and Tazobactam against Methicillin-Resistant Staphylococcus aureus, Antimicrob. Agents Chemother. 63 (2019) 10.1128/aac.02637-18. https://doi.org/10.1128/aac.02637-18.
[51] S. Gatadi, T.V. Lakshmi, S. Nanduri, 4(3H)-Quinazolinone derivatives: Promising antibacterial drug leads, Eur. J. Med. Chem. 170 (2019) 157–172. https://doi.org/10.1016/j.ejmech.2019.03.018.
[52] D.E. Nawrot, G. Bouz, O. Janďourek, K. Konečná, P. Paterová, P. Bárta, M. Novák, R. Kučera, J. Zemanová, M. Forbak, J. Korduláková, O. Pavliš, P. Kubíčková, M. Doležal, J. Zitko, Antimycobacterial pyridine carboxamides: From design to *in vivo* activity, Eur. J. Med. Chem. 258 (2023) 115617. https://doi.org/10.1016/j.ejmech.2023.115617.

[53] A. Daina, O. Michielin, V. Zoete, SwissADME: a free web tool to evaluate pharmacokinetics, drug-likeness and medicinal chemistry friendliness of small molecules, Sci. Rep. 7 (2017) 42717. https://doi.org/10.1038/srep42717.
[54] L.Z. Benet, C.M. Hosey, O. Ursu, T.I. Oprea, BDDCS, the Rule of 5 and Drugability, Adv. Drug Deliv. Rev. 101 (2016) 89–98. https://doi.org/10.1016/j.addr.2016.05.007.
[55] M.M. Hann, T.I. Oprea, Pursuing the leadlikeness concept in pharmaceutical research, Curr. Opin. Chem. Biol. 8 (2004) 255–263. https://doi.org/10.1016/j.cbpa.2004.04.003.
[56] S.N. Bolz, M.F. Adasme, M. Schroeder, Toward an Understanding of Pan-Assay Interference Compounds and Promiscuity: A Structural Perspective on Binding Modes, J. Chem. Inf. Model. 61 (2021) 2248–2262. https://doi.org/10.1021/acs.jcim.0c01227.
[57] N. Narimisa, N. Bostanghadiri, F. Goodarzi, S. Razavi, F.M. Jazi, Prevalence of Mycobacterium kansasii in clinical and environmental isolates, a systematic review and meta-analysis, Front. Microbiol. 15 (2024). https://doi.org/10.3389/fmicb.2024.1321273.
[58] V.O. Mussi, T.L.B.V. Simão, F.M. Almeida, E. Machado, L.D. de Carvalho, S.D. Calixto, G.A.M. Sales, E.C.Q. Carvalho, S.E.G. Vasconcellos, M. Catanho, P.N. Suffys, E.B. Lasunskaia, A Murine Model of Mycobacterium kansasii Infection Reproducing Necrotic Lung Pathology Reveals Considerable Heterogeneity in Virulence of Clinical Isolates, Front. Microbiol. 12 (2021) 718477. https://doi.org/10.3389/fmicb.2021.718477.
[59] K.M. Pennington, A. Vu, D. Challener, C.G. Rivera, F.N.U. Shweta, J.D. Zeuli, Z. Temesgen, Approach to the diagnosis and treatment of non-tuberculous mycobacterial disease, J. Clin. Tuberc. Mycobact. Dis. 24 (2021) 100244. https://doi.org/10.1016/j.jctube.2021.100244.
[60] S.M. Akram, P. Rawla, Mycobacterium kansasii Infection, in: StatPearls, StatPearls Publishing, Treasure Island (FL), 2024. http://www.ncbi.nlm.nih.gov/books/NBK430906/ (accessed May 13, 2024).